Literature Review

on

Quantum Control of Coherent Optical Responses in Gaseous and Solid Mediums

A report submitted in partial fulfillment of the requirements of Ph.D. Course Work

for the award of

Doctor of Philosophy in **Physics**

by

Rakiba Rahaman

Ph.D. Enrollment No. PHY211603

Under the Supervision of

Dr. Md. Mabud Hossain

Assistant Professor

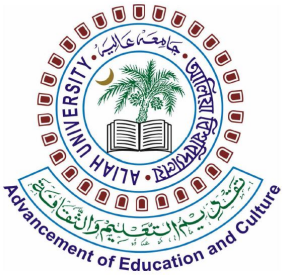

Department of Physics

Aliah University

Action Area II-A/27, New Town

Kolkata-160, India

2024

Declaration

I hereby declare that the report ***Literature Review on Quantum Control of Coherent Optical Responses in Gaseous and Solid Mediums*** submitted by me to the Department of Physics, **Aliah University**, Newtown, Kolkata - 700160 in partial fulfillment of the requirements of Ph.D. Course Work for the award of **Doctor of Philosophy** in **Physics** is a bona-fide record of the work carried out by me under the supervision of **Dr. Md. Mabud Hossain** during the period 2023-2024.

I further declare that all the materials used in this work are cited as far as possible.

(Signature)

Rakiba Rahaman

PHY211603

Department of Physics

Certificate

This is to certify that the report entitled ***Literature Review on Quantum Control of Coherent Optical Responses in Gaseous and Solid Mediums*** submitted by ***Rakiba Rahaman*** **(Roll No. PHY211603)** to **Aliah University**, in partial fulfullment of the requirement of Ph.D. Course Work for the award of the degree of **Doctor Of Philosophy** in **Physics** is a bona-fide work carried out under my supervision during the period 2023-2024. The review report fulfils the requirements as per the Ph.D. regulations of this University and in my opinion meets the necessary standards for submission.

(Signature)
Dr. Md. Mabud Hossain
(Ph.D. Supervisor)
Assistant Professor
Dept. of Physics, Aliah University

(Signature)
Prof.(Dr.) Sk. Faruque Ahmed
Professor, Head of the Department
Dept. of Physics, Aliah University

(Seal of the Department)

Date:

Place: Aliah University, Kolkata

Acknowledgements

I would like to deeply acknowledge the support and encouragement I have received from the people while completing this task. I want to express my sincere gratitude to all of them. First of all my sincere thanks go to my supervisor Dr. Md. Mabud Hossain, Assistant Professor, Department of Physics, Aliah University, for his initiative and constant inspiration. I would also like to thank Dr. Jayanta Kumar Saha and all the faculty members of Physics Department. I am really thankful to have some wonderful people as my seniors. It is really a joyful experience to be with them and learn from their experience. I would like to place my special thanks to my senior Dr. Aparajita Das and Samim Akhtar for their constant help and invaluable suggestions which enhanced my learning experience. I also want to thank all the research scholars of physics department of Aliah University. Lastly, I want to thank the West Bengal Minorities Development and Finance Corporation (WBMDFC) for providing Swami Vivekananda Merit-cum-Means Scholarship (SVMCMS) through Aliah University for financial support.

Rakiba Rahaman

PHY211603

Contents

1 Introduction **5**

2 Saturation Absorption Spectroscopy (SAS) **6**

2.1 Theoretical Calculation of SAS 7

3 Coherence population trapping (CPT) **11**

4 Electromagnetic induced transparency (EIT) **12**

4.1 EIT in Three-level System: Theoretical Modelling 13

4.1.1 Dynamics of the atom-laser coupled system 13

4.1.2 Λ-type system 14

4.1.3 Vee (V)-type system: 16

4.1.4 Cascade (Ξ)-type system: 17

5 Metamaterials **19**

5.1 Negative Index of Refraction 19

5.2 EIT in Metamaterials 21

5.2.1 Categories of EIT metamaterials 21

6 Surface plasmon polariton **22**

6.1 EIT in SPR system 23

7 Literature Survey **25**

7.1 Experimental Understandings 25

7.1.1 Experimental Observation 25

7.1.2 Further experimental advancements 27

7.2 Theoretical Understandings 29

7.2.1 Density matrix formalism 29

7.2.2 Other approaches 30

7.3 Metamaterials: 31

7.3.1 Theoretical concept (1968) 31

7.3.2 Experimental demonstration of NIM (Early to Mid 2000s) 31

7.3.3 EIT metamaterial 33

7.4 EIT-based Surface Plasmon Polariton : 34

8 Future outlook **35**

1 Introduction

The coherent interaction of light with the gaseous (*e.g.* atomic) medium is a fundamental research interest in atomic physics, quantum optics and quantum physics due to its immense applications in quantum information and quantum technology [1]. The coherent atomic medium provides a powerful platform for controlling light and photons, facilitating a wide range of applications in both classical and quantum optical communication and information processing. The coherent interaction leads to several phenomena like coherent population trapping (CPT) [2, 3], electromagnetic induced transparency (EIT) [4], electromagnetically induced absorption (EIA) [5], Autler-Townes (AT) splitting or AC stark splitting, lasing without inversion (LWI) [6]. These phenomena have several fundamental interests which are the paving stone of the many atomic physics applications. The coherent optical phenomena are based on quantum coherence and interference in an atomic medium. The interference between alternative transition pathways in quantum mechanical processes is a fascinating effect in non-linear quantum optics. Fano [7] first observed coherent optical phenomena in radiative transitions to atom-ionizing states. Coherent population trapping (CPT) is a notable laser-induced coherent optical phenomenon where resonant fluorescence or probe absorption decreases in the presence of a pump laser field. A closely related phenomenon to CPT is EIT, a quantum effect that modifies the optical properties of an atomic medium over a narrow frequency range, making it transparent to a probe field around the resonance frequency in the presence of a control laser beam. Another non-linear atomic coherent optical resonance is electromagnetically induced absorption (EIA), which is the opposite of EIT. EIA involves constructive quantum interference between two optical transition pathways caused by pump and probe laser fields, leading to increased initial absorption of the probe laser field over a small frequency range. The coherent optical phenomena effects such as CPT, EIT and EIA have attracted a lot of attention in very recent times due to their many useful applications in non-linear quantum optics such as quantum computation, optical information storage, development of atomic clocks magnetometer [8], light storage [9] and slowing-down fast light [10], laser without inversions [11], ion trapping [12] etc.

The study of coherent optical phenomena in solid mediums such as metamaterials and surface plasmon systems under EIT has also found an increased research interest. Metamaterials are artificial materials with a negative index of refraction, a property not found in natural materials, causing light to propagate in the opposite direction after refraction. Their unique optical properties stem from electromagnetic resonances due to their physical structure rather than their chemical composition. Initially proposed by Veselago [13] the existence of negative index materials was experimentally verified decades later by Pendry and Smith *et al.* [14]. This discovery sparked intense interest in metamaterials, which enable effects such as negative refraction, sub-wavelength focusing, EIT and electromagnetic cloaking. Recent research focuses on practical applications like sensing and modulators. Besides,

coherent control of optical phenomena for surface plasmon polaritons (SPPs) at a metal surface is also possible based on the EIT [15]. The SPPs [16] are surface charge density oscillations of free electrons in metals, where photons couple to conducting electron excitations. Primarily used in nano-optics, SPPs enable light manipulation at sub-wavelength scales, facilitating applications in chemical and biological sensors [17, 18, 19] and optical circuits [20]. These advancements support the miniaturization of modern chip technology.

2 Saturation Absorption Spectroscopy (SAS)

In conventional laser spectroscopy, the closely spaced spectral lines arising from the hyperfine structure of the atomic system are often not resolved properly due to the Doppler broadening effect, which is result of the thermal velocity distribution of atoms at room temperature. In the early 1970s, Schawlow and Hansch [21] developed a practical way to use the nonlinear interaction of laser light with atoms to produce spectra without Doppler broadening. Their technique, known as laser-saturated absorption spectroscopy, grew out of fundamental work on nonlinear optics done by them and other physicists e.g., Bloembergen, Lamb, and Javan [22]. The Maxwell velocity distribution results in an absorption profile with Gaussian lineshape which is due to inhomogeneous broadening. The Doppler linewidth for ^{87}Rb atoms at room temperature on D_2 line at 780 nm is about 600 MHz and the natural linewidth of individual hyperfine transitions is only 6 MHz. The standard method to resolve such a narrow transition is adapting the technique of Saturation Absorption Spectroscopy. The basic experimental setup for SAS is shown schematically in figure (1). Here the source laser beam is split into two beams,

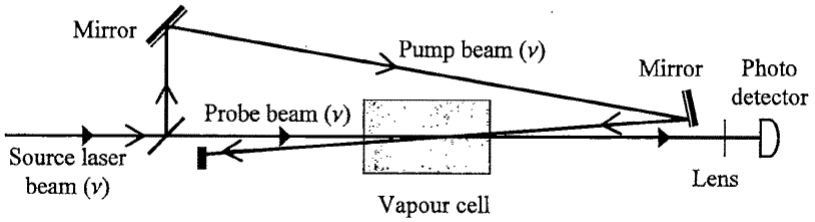

Figure 1: Basic experimental setup for SAS [23].

the first is the weak transmitted beam (probe beam) and the second is a much stronger reflected beam (pump beam) which counter propagates with respect to the probe and plays the role of saturating the transition. A photodetector measures the absorption of the weak transmitted beam.

Consider the laser frequency ν slightly below ν_0 (resonance frequency). In this case, the probe beam will interact with the atoms moving towards it since they will see the radiation is blue shifted to ν_0 due to the Doppler effect. Similarly, the atoms moving in opposite directions i.e., moving towards

the pump beam, will interact with the pump beam. For $\nu > \nu_0$ we can explain the situation similarly as before however here the frequency will be red-shifted. So at any given frequency (other than $\nu = \nu_0$), both beams can only interact with the atoms traveling in opposite directions but with equal speed. Therefore the presence of one beam does not affect the other beam. When the laser frequency (ν) is in resonance with the transition frequency (ν_0) i.e., $\nu = \nu_0$ both pump and probe beam will interact with the same velocity class atoms which do not move parallel to the beams i.e., $v_z = 0$. In that case

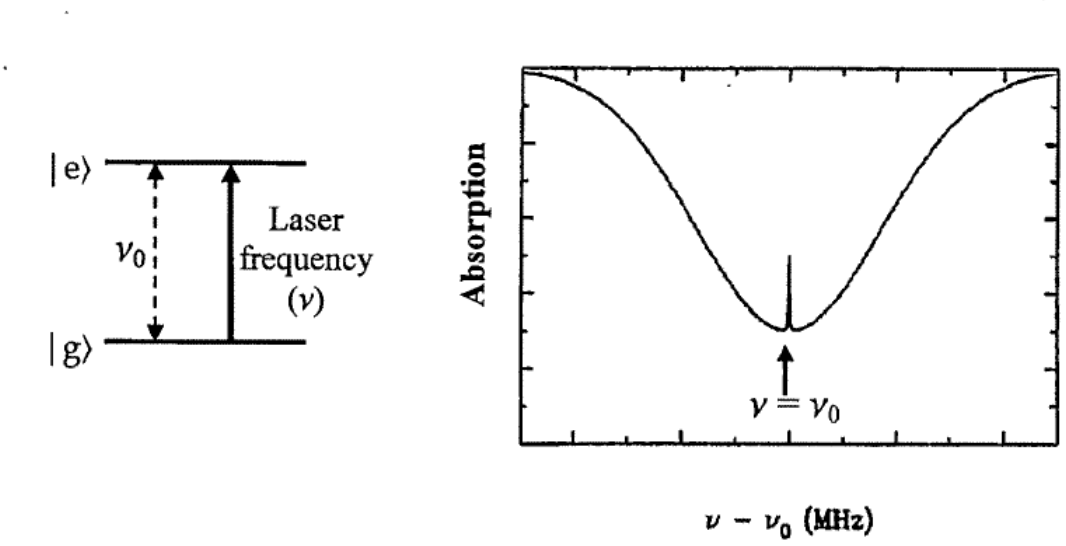

Figure 2: Probe absorption spectrum of two level atomic system under SAS configuration [23].

the high-intensity pump beam will cause the atoms to make the transition into excited state leading to a high absorption rate [if the pump beam is strong enough, half of the atoms would be in excited state in no time and there would be identically zero probe absorption i.e., those atoms are completely saturated by the pump beam. Hence the name Saturation Absorption Spectroscopy]. As a result, the absorption is reduced compared to the pump beam and we see a sharp dip in the absorption spectrum of the probe beam for $v_z = 0$. This dip is referred to as Lamb Dip [24] (see Fig. 2).

2.1 Theoretical Calculation of SAS

In SAS, two counter-propagating laser beams from the same source are sent through the atomic sample. A standing wave is formed by these counter-propagating beams. Here the moving atoms interact with two oppositely moving waves and this interaction will create two holes by each wave depending upon the detuning. The field inside the cavity is described by a standing wave

$$E(z,t) = E_0 \cos \nu t \ \sin kz \tag{1}$$

The total Hamiltonian of the system H is given by the sum of the perturbed Hamiltonian H_0 and the atom–field interaction Hamiltonian H_I

$$H = H_0 + H_I \tag{2}$$

where

$$H_0 = \hbar\omega_a|a\rangle\langle a| + \hbar\omega_b|b\rangle\langle b| \tag{3}$$

Here $|a\rangle$ and $|b\rangle$ are the ground state and excited state respectively.

$$H_I = -\vec{\mu}.\vec{E}(z,t) \tag{4}$$

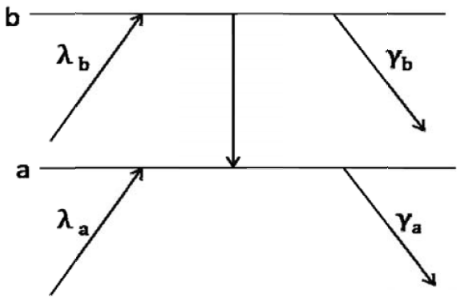

Figure 3: Two level atom showing pumping (λ_a and λ_b and population decay (γ_a and γ_b)) [23].

The density matrix for two level atomic system is written as,

$$\rho = \begin{bmatrix} \rho_{aa} & \rho_{ab} \\ \rho_{ba} & \rho_{bb} \end{bmatrix} \tag{5}$$

The time evolution density matrix equation (master equation) is given by,

$$\frac{d}{dt}(\rho_{ij}) = -\frac{i}{\hbar}\sum[H_{ik}\rho_{kj} - \rho_{ik}H_{kj}] + L(\hat{\rho}) \tag{6}$$

where $L(\hat{\rho})$ is the Lindblad relaxation term. This team can be written as,

$$L(\hat{\rho}) = -\frac{\Gamma_{ij}}{2}\{\hat{\sigma}_{+ij}\hat{\sigma}_{-ij}\hat{\rho} - 2\hat{\sigma}_{-ij}\hat{\rho}\hat{\sigma}_{+ij} + \hat{\rho}\hat{\sigma}_{+ij}\hat{\sigma}_{-ij}\} \tag{7}$$

where $\{i,j\} \in \{\{a,b\},\{b,a\}$, $\hat{\sigma}_{+ij} = |i\rangle\langle j|$, $\hat{\sigma}_{-ij} = |j\rangle\langle i|$ and γ_{ij} are the spontaneous transition rates between the states i and j. In our case, $\frac{d}{dt}$ can be written as

$$\frac{d}{dt} = \frac{\partial}{\partial t} + v\frac{\partial}{\partial z} \tag{8}$$

where v is the velocity of the atom.

After using rotating wave approximation (RWA) and slowly varying envelope approximation (SVEA), the rate of the change of the density matrix is given by,

$$\left(\frac{\partial}{\partial t}+v\frac{\partial}{\partial z}\right)\rho_{bb} = (\lambda_b-\gamma_b\rho_{bb})-i\frac{\mu E_0}{2\hbar}\sin kz\ (\tilde{\rho}_{ba}-\tilde{\rho}_{ab}) \tag{9}$$

$$\left(\frac{\partial}{\partial t}+v\frac{\partial}{\partial z}\right)\rho_{aa} = (\lambda_a-\gamma_a\rho_{aa})+i\frac{\mu E_0}{2\hbar}\sin kz\ (\tilde{\rho}_{ba}-\tilde{\rho}_{ab}) \tag{10}$$

$$\left(\frac{\partial}{\partial t}+v\frac{\partial}{\partial z}\right)\tilde{\rho}_{ba} = -(i\Delta+\gamma_{ba})\tilde{\rho}_{ba}-i\frac{\mu E_0}{2\hbar}\sin kz\ (\rho_{bb}-\rho_{aa}) \tag{11}$$

$$\left(\frac{\partial}{\partial t}+v\frac{\partial}{\partial z}\right)\tilde{\rho}_{ab} = (i\Delta-\gamma_{ab})\tilde{\rho}_{ab}+i\frac{\mu E_0}{2\hbar}\sin kz\ (\rho_{bb}-\rho_{aa}) \tag{12}$$

where $\rho_{ab}=\tilde{\rho_{ab}}e^{i\nu t}$, $\rho_{ba}=\tilde{\rho_{ba}}e^{-i\nu t}$, $e^{\pm i\nu t}\cos\nu t=\frac{1}{2}$ and $\Delta=(\omega_{ba}-\nu)$ is the detuning.

From physical considerations, we can consider the lowest order effect to be the sum of the effect caused by each wave separately. The induced dipole moment caused by the interaction of the two waves can be written as

$$\tilde{\rho}_{ba}=\rho_+e^{ikz}+\rho_-e^{-ikz} \tag{13}$$

We assume that the off-diagonal term reach their equilibrium values much faster than the diagonal element, so that $\frac{d}{dt}\rho_\pm=0$. Finally we can can find [23, 24]

$$\rho_{bb}-\rho_{aa}=\frac{\bar{N}}{1+\frac{I\eta}{2[L(\Delta+kv)+L(\Delta-kv)]}} \tag{14}$$

where L is the dimensionless Lorentzian function, $\bar{N}$ is the unperturbed population difference, I is the dimensionless field intensity and η is the saturation decay parameter.

$$L(\Delta\pm kv)=\frac{\gamma_{ba}^2}{\gamma_{ba}^2+(\Delta\pm kv)^2}$$

$$\bar{N}=\frac{\lambda_b}{\gamma_b}-\frac{\lambda_a}{\gamma_a}$$

$$I=\frac{1}{2\gamma_b\gamma_a\left(\frac{\mu E_0}{\hbar}\right)^2}$$

$$\eta=\frac{\gamma_a+\gamma_b}{2\gamma_{ba}}$$

The unsaturated population difference $\bar{N}$ is described by a Gaussian distribution function. Hence, the population difference given by equation eqn. (14) is a Gaussian function with two holes described by the Lorentzian function centered at $v=\pm\frac{(\omega_{ba}-\nu)}{k}$ and with a width of γ_{ba}. In this figure 4. the holes (known as a Bennet hole) are situated at $v=\pm\frac{\Delta}{k}$ and their height are determined by the field

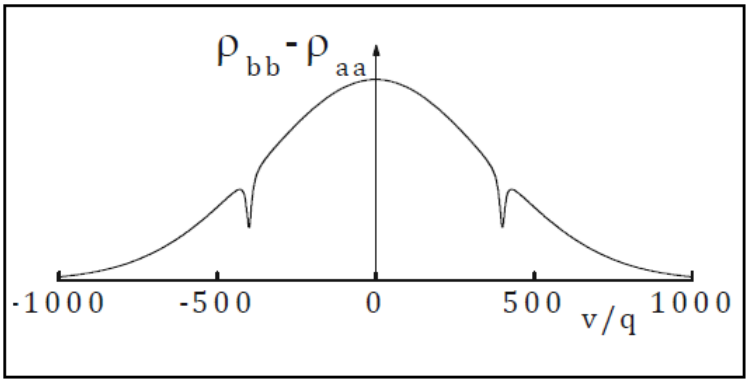

Figure 4: The holes (Bennet holes) created by the oppositely running waves in the velocity distribution curve [23]

intensity I and the saturation parameter η. With increase of detuning, the holes move away from each other until they reach the trail of the velocity distribution curves. When the detuning is small, they approach each other and the two holes may overlap at resonance. We noted that if the detuning is reduced, the two Bennet holes burnt on the velocity distribution curve approach each other. When the detuning eventually goes to zero the holes coincide and a strong dip appears. This is called Lamb dip [24] (see Fig. 5). The dip has a width comparable to the natural width of the transition

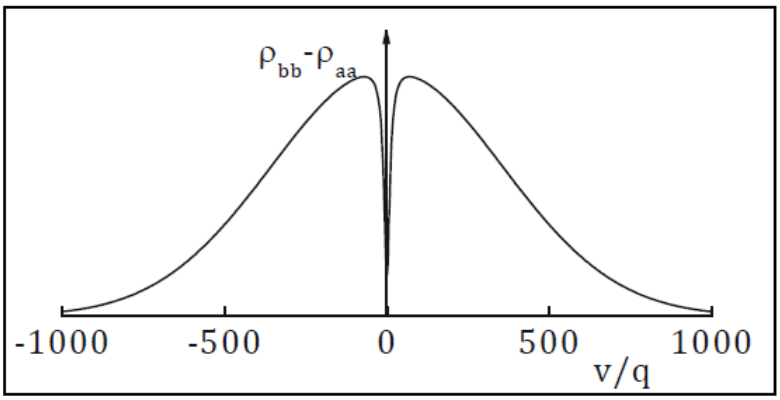

Figure 5: Lamb dip at the central frequency where the two holes merge together at resonance [23].

and can be used for the measurement of hyperfine transition frequency. If there are closely spaced transitions within frequency spacing much smaller than the Doppler width they cannot be resolved in a single-wave laser spectroscopy. But they can be easily resolved in the standing wave.

3 Coherence population trapping (CPT)

Coherence population trapping (CPT) was first experimentally observed by Alzetta *et al.* [2] . They observed nonabsorption resonances when the fluorescent light of sodium vapor illuminated by a multimode laser field was analyzed as a function of the applied magnetic field. It was found that a steady decrease in fluorescence intensity occurs when some hyperfine transitions of the ground state match the frequency difference of the two laser modes. Above phenomena was termed as CPT which was a result of the nonlinear effects of coherence and interference due to simultaneous excitation pathways.

A three-level atomic system with two closely spaced ground levels when optically coupled to a third common excited state via two external coherent laser fields, the atomic population trapped in a coherent superposition of ground state. This phenomena occurs only when certain condition matched and that is the frequency difference between two external fields matches with the separation between two ground state energy levels. Some prominent applications of CPT are lasing without inversion and efficient transfer of population from one state to other state.

Theoretical understanding of CPT: To understand CPT, we consider the atom to be in Λ configuration (figure 6) in which two lower levels $|1\rangle$ and $|2\rangle$ are coupled to a common excited state $|3\rangle$ by two near-resonance laser fields of strengths Ω_c (laser frequency ω_c) and Ω_p (laser frequency (ω_p). The laser field strength is defined as the Rabi frequency $\Omega = \frac{\mu\zeta}{\hbar}$, where μ is the transition dipole moment and ζ is the electric field amplitude. The laser frequency detunings are $\Delta_c(\omega_c - \omega_{23})$ and $\Delta_p(\omega - \omega_{13})$, where ω_{23} and ω_{13} are the atomic transition frequencies of the transitions $|2\rangle \leftrightarrow |3\rangle$ and $|1\rangle \leftrightarrow |3\rangle$ respectively. The two-photon frequency detuning is $\Delta = \Delta_c - \Delta_p$. The Hamiltonian for the

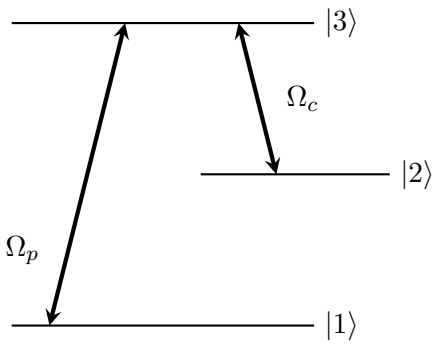

Figure 6: Lambda (Λ) type system

system under RWA can be written as

$$H = H_0 + H_I \tag{15}$$

where H_0 is the unperturbed Hamiltonian,

$$H_0 = \hbar\omega_1|1\rangle + \hbar\omega_2|2\rangle + \hbar\omega_3|3\rangle \tag{16}$$

and H_I is the atom-laser interaction Hamiltonian,

$$H_I = -\frac{\hbar}{2}[(|1\rangle\langle 3|\Omega_p e^{-i\omega_p t}) + (|2\rangle\langle 3|\Omega_c e^{-i\omega_c t}) + C.C.] \tag{17}$$

At the two-photon resonance condition ($\Delta = 0$), two of the eigenstates of the total Hamiltonian (H) will be the coherent superposition of the two ground states ($|1\rangle$ and $|2\rangle$) of the bare atom basis as follows:

$$|+\rangle = \frac{\Omega_p}{\Omega'}|1\rangle + \frac{\Omega_c}{\Omega'}|2\rangle \tag{18}$$

$$|-\rangle = \frac{\Omega_c}{\Omega'}|1\rangle - \frac{\Omega_p}{\Omega'}|2\rangle \tag{19}$$

where $\Omega' = (\Omega_c^2 + \Omega_p^2)$. Now, the state described above does not contain upper level $|3\rangle$. That means the atomic population is trapped in the lower levels and there is no absorption even if the field is present. Since the state $|-\rangle$ is nonabsorbing, it is called the 'dark' or 'trapped' or 'non-coupled' state. This coherent trapping phenomenon arises due to the destructive quantum interference between the atomic transition from $|1\rangle$ to $|3\rangle$ and $|2\rangle$ to $|3\rangle$. If the two laser field strengths become nearly equal ($\Omega_c \approx \Omega_p$), the transition moment between the dark state $|-\rangle$ and the excited state $|3\rangle$ vanishes and the atoms get trapped in the dark state $|-\rangle$ by the spontaneous emission via the state $|3\rangle$. This is the CPT effect which made the suppression of fluorescence in the first two experiments done by Alzetta *et al.* and Gray *et al.* [2, 25].

4 Electromagnetic induced transparency (EIT)

A very closely related coherence phenomenon to CPT is EIT. EIT or Electromagnetic induced transparency is a quantum phenomenon which make use of a resonant electromagnetic field to alter the optical properties of an atomic medium. Under resonance condition, the atoms will absorb energy from surroundings and excite to the higher energy state. Here in EIT, two different beams are sent through the medium, one is a weak probe beam and the other is a highly intense pump or control beam ($\Omega_p << \Omega_c$), each resonant with a distinct atomic transition. The joint effect of these two beams alters the absorption spectrum which now includes an optical window at resonant frequency where the medium exhibits high transparency. Hence the name Electromagnetic induced transparency. In addition to that, we get a highly enhanced nonlinear susceptibility in this optical window which gives rise to many useful application including effective nonlinear mixing, slow light and lasing without

inversion. EIT was first theoretically explained by Harris *et al.* [26] in 1990 and Boller *et al.* [27] reported the first experimental observation of EIT resonance in a Λ type system in 1991. In order to understand the EIT phenomenon, it is necessary to examine how the coherent light interacts with an atomic system.

4.1 EIT in Three-level System: Theoretical Modelling

A three-level system is a system with an effective superposition of two two-level systems. Unlike a two-level system, the three-level system presents choices in arranging the energy levels and driving fields. According as the shape of allowed transition lines in the schematic energy level diagram three main classes of level scheme can be considered. These basic three atom-laser coupling schemes are Lambda (Λ)-type, Vee (V)-type and Cascade (Ξ)-type atomic system.

4.1.1 Dynamics of the atom-laser coupled system

The total Hamiltonian (H) for an atom-laser coupled system is given by,

$$H = H_0 + H_I \tag{20}$$

where H_0 is the Hamiltonian of bare atomic system and H_I is interaction Hamiltonian of atom-laser coupling.

The density matrix of the atomic system is

$$\rho = \begin{bmatrix} \rho_{11} & \rho_{12} & \rho_{13} \\ \rho_{21} & \rho_{22} & \rho_{23} \\ \rho_{31} & \rho_{32} & \rho_{33} \end{bmatrix} \tag{21}$$

For a three-level system, the Optical Bloch Equations can be obtained by the following formula (22),

$$\dot{\rho}_{ij} = -\frac{i}{\hbar}\sum[H_{ik}\rho_{kj} - \rho_{ik}H_{kj}] + L(\hat{\rho}) \tag{22}$$

where $L(\hat{\rho})$ is the Lindblad relaxation term. This team can be written as,

$$L(\hat{\rho}) = -\frac{\Gamma_{ij}}{2}\{\hat{\sigma}_{+ij}\hat{\sigma}_{-ij}\hat{\rho} - 2\hat{\sigma}_{-ij}\hat{\rho}\hat{\sigma}_{+ij} + \hat{\rho}\hat{\sigma}_{+ij}\hat{\sigma}_{-ij}\} \tag{23}$$

where $\{i,j\} \in \{\{1,2\},\{2,1\},\{2,3\},\{3,2\},\{1,3\},\{3,1\}\}$, $\hat{\sigma}_{+ij} = |i\rangle\langle j|$, $\hat{\sigma}_{-ij} = |j\rangle\langle i|$ and Γ_{ij} are the spontaneous transition rates between the states i and j.

4.1.2 Λ-type system

The three-level Λ-type system is formed by the two ground levels ($|1\rangle$ and $|2\rangle$) coupled to a common excited level ($|3\rangle$) as depicted in figure (7) . Here the transitions between these two ground levels $|1\rangle$ and $|2\rangle$ are dipole forbidden. The upper ground level $|2\rangle$ is coupled to the excited level $|3\rangle$ by the strong pump laser field of frequency ω_c and the levels $|1\rangle$ and $|3\rangle$ are coupled by the weak probe laser field of frequency ω_p. The Ω_c and Ω_p are the Rabi frequencies of the pump and probe laser fields respectively. The pump field strength Ω_c is assumed to be much greater than the probe field strength Ω_p i.e., $\Omega_c > \Omega_p$.

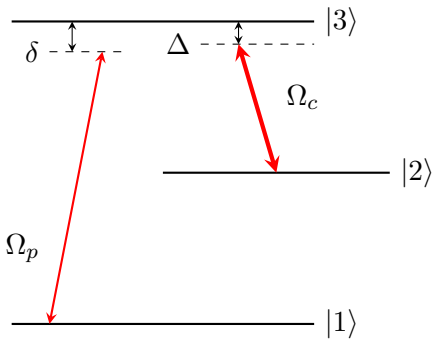

Figure 7: Lambda (Λ)- type atom-laser interaction system

After using rotating wave approximation (RWA) and slowly varying envelope approximation (SVEA), the Optical Bloch equations (OBEs) for a Λ- type system becomes,

$$\begin{aligned}
\dot{\tilde{\rho}}_{11} &= \frac{i\Omega_p}{2}(\tilde{\rho}_{31} - \tilde{\rho}_{13}) + \Gamma_{21}(\tilde{\rho}_{22} - \tilde{\rho}_{11}) + \Gamma_{31}\tilde{\rho}_{33} \\
\dot{\tilde{\rho}}_{22} &= \frac{i\Omega_c}{2}(\tilde{\rho}_{32} - \tilde{\rho}_{23}) - \Gamma_{21}(\tilde{\rho}_{22} - \tilde{\rho}_{11}) + \Gamma_{32}\tilde{\rho}_{33} \\
\dot{\tilde{\rho}}_{33} &= \frac{i\Omega_p}{2}(\tilde{\rho}_{13} - \tilde{\rho}_{31}) + \frac{i\Omega_c}{2}(\tilde{\rho}_{23} - \tilde{\rho}_{32}) - (\Gamma_{32} + \Gamma_{31})\tilde{\rho}_{33} \\
\dot{\tilde{\rho}}_{21} &= [i(\delta - \Delta) - \gamma_{21}]\tilde{\rho}_{21} + \frac{i\Omega_c}{2}\tilde{\rho}_{31} - \frac{i\Omega_p}{2}\tilde{\rho}_{23} \\
\dot{\tilde{\rho}}_{31} &= [i\delta - \gamma]\tilde{\rho}_{31} + \frac{i\Omega_p}{2}(\tilde{\rho}_{11} - \tilde{\rho}_{33}) + \frac{i\Omega_c}{2}\tilde{\rho}_{21} \\
\dot{\tilde{\rho}}_{32} &= [i\Delta - \gamma]\tilde{\rho}_{32} + \frac{i\Omega_c}{2}(\tilde{\rho}_{22} - \tilde{\rho}_{33}) + \frac{i\Omega_p}{2}\tilde{\rho}_{12}
\end{aligned} \tag{24}$$

Δ and δ are the pump and probe detuning respectively.
The decay terms are, $\gamma_{21} = \frac{\Gamma_{21}+\Gamma_{12}}{2}$, $\gamma = \frac{\Gamma_{21}+\Gamma_{31}+\Gamma_{32}}{2}$.

Analytical solution of OBEs: The steady state solution for $\tilde{\rho}_{31}$ for weak probe (i.e $\Omega_P^2 = 0$) is given by,

$$\tilde{\rho}_{31} = \frac{-\frac{i\Omega_P}{2}}{(\gamma - i\delta) + \frac{\frac{\Omega_C^2}{4}}{\gamma_{21} - i(\delta - \Delta)}} \tag{25}$$

The diagonal elements of $\rho_{ii}(i = 1, 2, 3)$ represent the atomic population of the corresponding levels, while the off-diagonal elements ρ_{ij} $(i \neq j)$ represent the atomic coherence induced by the pump-probe laser fields among the different levels. To understand the modification of the optical properties (absorption and dispersion) of an atomic medium dressed by the laser fields, we need to find out the optical susceptibility which is related to the macroscopic polarization as,

$$P(\omega) = \varepsilon_0 \chi(\omega) \zeta \tag{26}$$

Here ε_0 is the permittivity of the vacuum and the macroscopic polarization $P(\omega)$ is related to the microscopic atomic coherence ρ_{ij} at the transition frequency ω as,

$$P(\omega) = N \mu_{ij} \rho_{ij} \tag{27}$$

where N is the atomic number density. So the complex susceptibility can be written as

$$\chi = \chi^{'} + i\chi^{''} = \frac{N|\mu_{ij}|^2 \rho_{ij}}{\hbar \varepsilon_0 (\Omega_p)_{ij}} \tag{28}$$

The imaginary part $(\chi^{''})$ gives the absorption properties of the medium; where the real part $(\chi^{'})$ describes the dispersive properties of the medium and it can be shown that the $Im[\rho_{ij}]$ and $Re[\rho_{ij}]$ is directly proportional to $Im[\chi]$ and $Re[\chi]$ respectively.

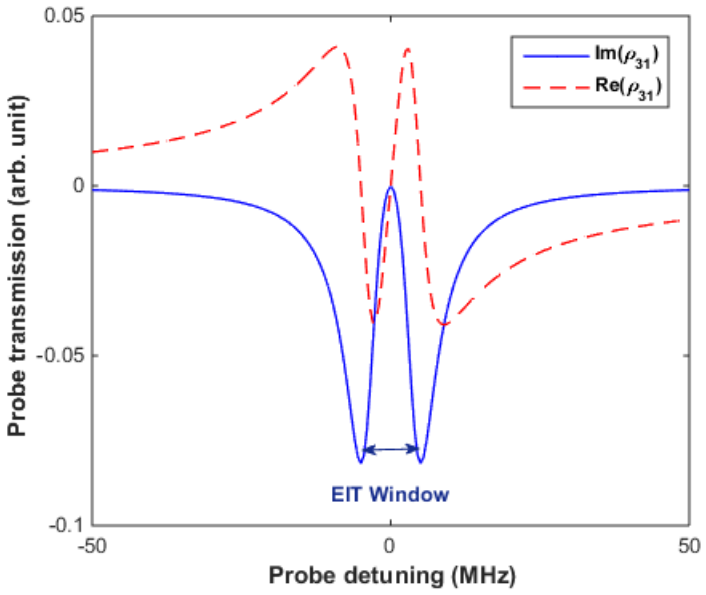

Figure 8: Real and imaginary part of $\tilde{\rho}_{31}$ vs probe detuning (δ) for Λ-type system

4.1.3 Vee (V)-type system:

Vee (V) type system is formed when the ground level ($|1\rangle$) and middle level ($|2\rangle$) are coupled by a strong pump beam. The upper level ($|3\rangle$) is coupled to the lower level ($|1\rangle$) by a weak probe beam.. Here the transitions between upper and middle levels $|3\rangle$ and $|2\rangle$ are dipole forbidden. The Ω_c and Ω_p are the Rabi frequencies of the pump and probe laser fields respectively. After using rotating

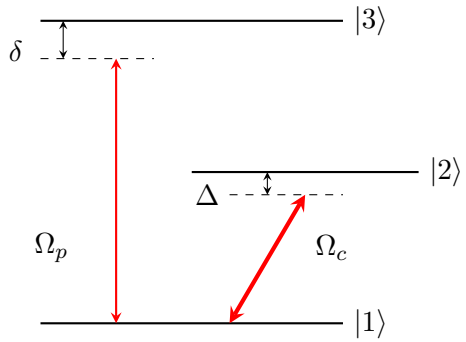

Figure 9: Vee (V)- type atom-laser interaction system

wave approximation (RWA) and slowly varying envelope approximation (SVEA), the Optical Bloch equations for a V-type system become,

$$\begin{aligned}
\dot{\tilde{\rho}}_{11} &= \frac{i\Omega_p}{2}(\tilde{\rho}_{31} - \tilde{\rho}_{13}) + \frac{i\Omega_c}{2}(\tilde{\rho}_{21} - \tilde{\rho}_{12}) + \Gamma_{21}\tilde{\rho}_{22} + \Gamma_{31}\tilde{\rho}_{33} \\
\dot{\tilde{\rho}}_{22} &= \frac{i\Omega_c}{2}(\tilde{\rho}_{12} - \tilde{\rho}_{21}) - \Gamma_{21}\rho_{22} \\
\dot{\tilde{\rho}}_{33} &= \frac{i\Omega_c}{2}(\tilde{\rho}_{13} - \tilde{\rho}_{31}) + \Gamma_{31}\tilde{\rho}_{33} \\
\dot{\tilde{\rho}}_{21} &= [i\delta - \Gamma_{21}]\tilde{\rho}_{21} + \frac{i\Omega_c}{2}(\tilde{\rho}_{11} - \tilde{\rho}_{22}) - \frac{i\Omega_p}{2}\tilde{\rho}_{23} \\
\dot{\tilde{\rho}}_{31} &= [i\delta - \frac{\Gamma_{21}}{2}]\tilde{\rho}_{31} + \frac{i\Omega_p}{2}(\tilde{\rho}_{11} - \tilde{\rho}_{33}) - \frac{i\Omega_c}{2}\tilde{\rho}_{32} \\
\dot{\tilde{\rho}}_{32} &= [i(\delta - \Delta) - \frac{(\Gamma_{21} + \Gamma_{31})}{2}]\tilde{\rho}_{32} + \frac{i\Omega_p}{2}\tilde{\rho}_{12} - \frac{i\Omega_c}{2}\tilde{\rho}_{31}
\end{aligned} \tag{29}$$

Δ and δ are the pump and probe detuning respectively.

Analytical solution of OBEs: Under weak probe approximation ($|\Omega_p| << |\Omega_c|$) the steady state solution for OBEs is given by,

$$\tilde{\rho}_{31} = \frac{\frac{\Omega_p}{2}}{\frac{\frac{\Omega_c^2}{4}}{(\delta-\Delta)+\frac{i(\Gamma_{21}+\Gamma_{31})}{2}} - (\delta + \frac{i\Gamma_{31}}{2})} \tag{30}$$

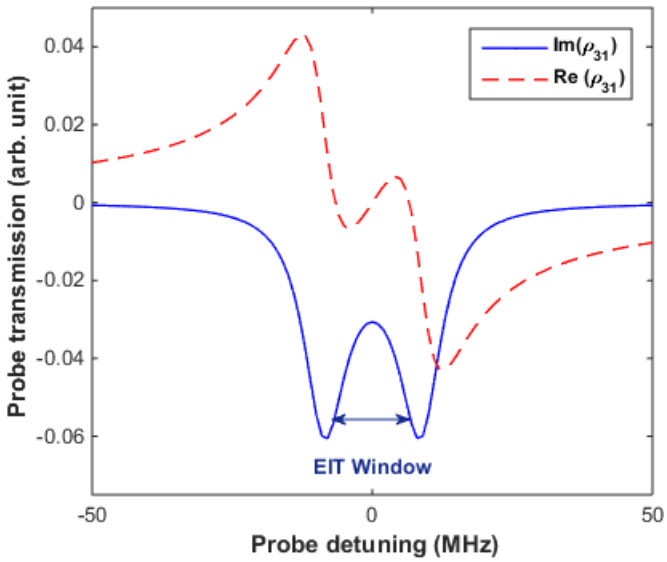

Figure 10: Real and imaginary part of $\tilde{\rho}_{31}$ vs probe detuning (δ) for Vee (V) type system

4.1.4 Cascade (Ξ)-type system:

In cascade (Ξ) type system lower ($|1\rangle$) and middle energy level ($|2\rangle$) are connected by weak probe field and middle ($|2\rangle$) and upper level ($|3\rangle$) are coupled by strong control or pump beam. The transition between upper and lower level is dipole forbidden.

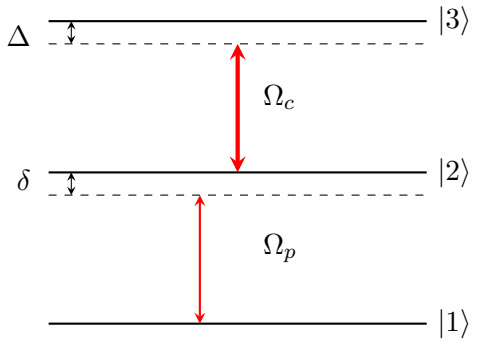

Figure 11: Cascade (Ξ)- type atom-laser interaction system

Using RWA and SVEA, the Optical Bloch Equations for a cascade (Ξ) type system become,

$$\begin{aligned}
\dot{\tilde{\rho}}_{11} &= \frac{i\Omega_p}{2}(\tilde{\rho}_{21} - \tilde{\rho}_{12}) + \Gamma_{21}\tilde{\rho}_{22} \\
\dot{\tilde{\rho}}_{22} &= \frac{i\Omega_p}{2}(\tilde{\rho}_{12} - \tilde{\rho}_{21}) + \frac{i\Omega_c}{2}(\tilde{\rho}_{32} - \tilde{\rho}_{23}) - \Gamma_{21}\rho_{22} + \Gamma_{32}\rho_{33} \\
\dot{\tilde{\rho}}_{33} &= \frac{i\Omega_c}{2}(\tilde{\rho}_{23} - \tilde{\rho}_{32}) - \Gamma_{32}\tilde{\rho}_{33} \\
\dot{\tilde{\rho}}_{21} &= [i\delta - \frac{\Gamma_{21}}{2}]\tilde{\rho}_{21} + \frac{i\Omega_p}{2}(\tilde{\rho}_{11} - \tilde{\rho}_{22}) - \frac{i\Omega_c}{2}\tilde{\rho}_{31} \\
\dot{\tilde{\rho}}_{31} &= [i(\delta + \Delta) - \frac{\Gamma_{32}}{2}]\tilde{\rho}_{31} - \frac{i\Omega_p}{2}\tilde{\rho}_{32} + \frac{i\Omega_c}{2}\tilde{\rho}_{21} \\
\dot{\tilde{\rho}}_{32} &= [i\Delta - \frac{(\Gamma_{21} + \Gamma_{32})}{2}]\tilde{\rho}_{32} + \frac{i\Omega_c}{2}(\tilde{\rho}_{22} - \tilde{\rho}_{33}) - \frac{i\Omega_p}{2}\tilde{\rho}_{31}
\end{aligned} \tag{31}$$

Analytical solution of OBEs: Under weak probe approximation ($|\Omega_p| << |\Omega_c|$) the steady state solution for OBEs is given by,

$$\tilde{\rho}_{21} = \frac{\frac{\Omega_p}{2}}{\frac{\frac{\Omega_c^2}{4}}{(\delta+\Delta)+\frac{i\Gamma_{32}}{2}} - (\delta + \frac{i\Gamma_{21}}{2})} \tag{32}$$

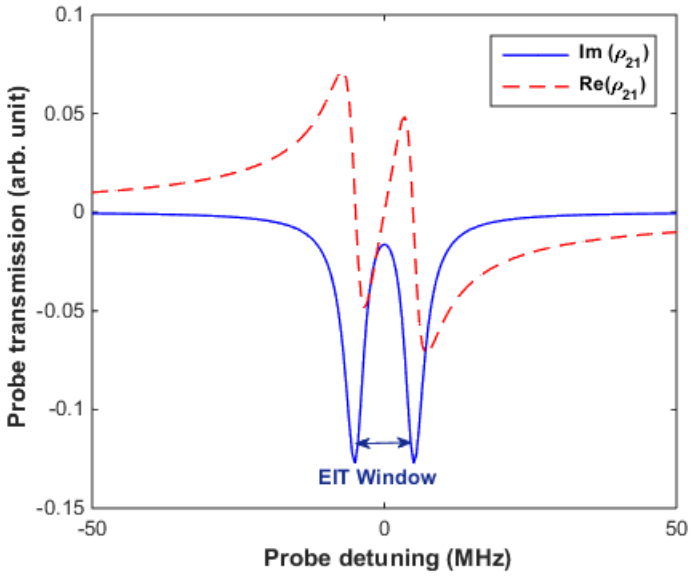

Figure 12: Real and imaginary part of $\tilde{\rho}_{21}$ Vs probe detuning (δ) for Cascade Ξ type system

5 Metamaterials

Metamaterials refer to a class of artificial materials with constituent unit cells structured at a size smaller than the wavelength of the electromagnetic radiation at which they are meant to operate. Their optical properties arise from electromagnetic resonances resulting from the physical structure of sub-wavelength elements. The metamaterials are also called as left-handed (LH) materials or backward wave (BW) media or negative index materials (NIM) or double negative (DNG) media. In addition, metamaterials have some special properties such as perfect lensing, classical electromagnetically induced transparency, cloaking capability, high frequency magnetism etc.

5.1 Negative Index of Refraction

Index of refraction is a fundamental constant of material which describes the interaction between electromagnetic radiation and matter. It has been considered as intrinsic property of material, quantifies how fast a light travels through the material. Refractive index is a complex quantity ($n = n' + in''$). For all naturally occurring material, the real value of refractive index (n') is always a positive quantity (in general, $n \geq 1$).

The optical properties of materials are governed by two material constants, the permittivity ϵ and the permeability μ, describing the coupling of a material to the electric and magnetic field components of light respectively. The relation between refractive index (n), relative permittivity (ϵ) and relative permeability (μ) is given by,

$$n = \sqrt{\epsilon\mu} \tag{33}$$

When either permittivity or permeability is negative, refraction index becomes a imaginary quantity and EM wave cannot pass through the material. Imaginary value of n leads to exponentially decaying waves (evanescent wave) instead of propagating waves. Such materials are either metal or magnet. On the other hand, when both permittivity and permeability are positive or negative, the refractive index has a real value and the electromagnetic wave can transmit through them.

A possible approach to achieve the negative RI in a passive medium is to design a material where the (isotropic) permittivity $\epsilon = \epsilon' + i\epsilon''$ and the (isotropic) permeability $\mu = \mu' + i\mu''$ obey the inequality,

$$\epsilon'|\mu| + \mu'|\epsilon| < 0 \tag{34}$$

This leads to a negative real part of the refractive index. Relation (34) is satisfied if $\epsilon' < 0$ and $\mu' < 0$.

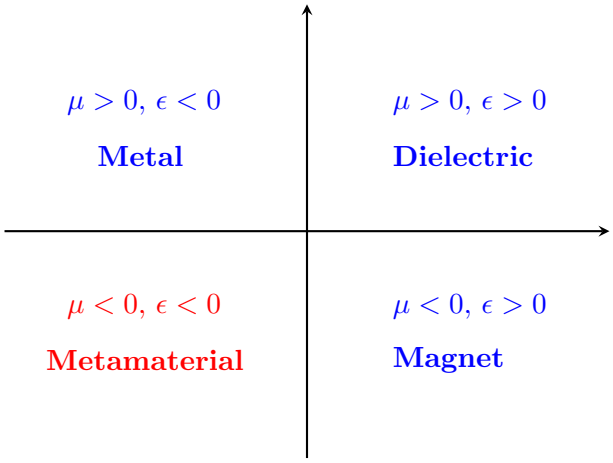

Figure 13: Permittivity and permeability diagram

The relation between electric field $\vec{E}$, magnetic field $\vec{M}$ and wave vector $\vec{k}$ is written as,

$$\vec{B} = \frac{(\vec{k} \times \vec{E})}{\omega} \tag{35}$$

and the Poynting vector is given by;

$$\vec{S} = \frac{(\vec{E} \times \vec{B})}{c} \tag{36}$$

From eqs. (35) and (36), it is clear that in a positive-index material with positive ϵ and μ, the wave vector $\vec{k}$ and the electric and magnetic field vectors $\vec{E}$ and $\vec{B}$ form a right-handed set. However, in a negative index material where ϵ and μ are both negative the $\vec{k}$, $\vec{E}$, and $\vec{B}$ vectors form a left-handed set. In that case, the wave vector $\vec{k}$, which represents the direction of propagation of phase fronts, and the Poynting vector $\vec{S}$ which represents the direction of energy flow are antiparallel. Thus, if we

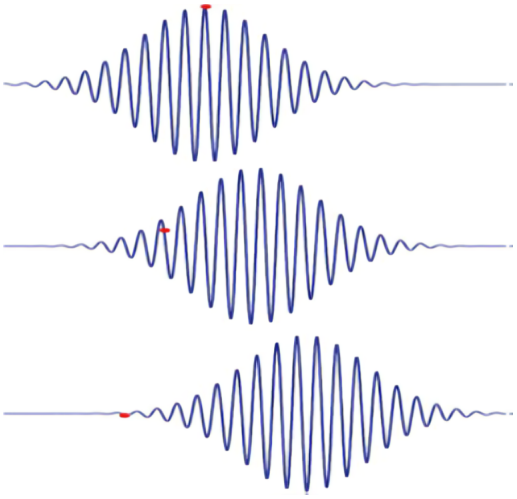

Figure 14: Propagation of a Gaussian wave packet in a negative-index material as time proceeds. The envelope of the packet propagates to the right, whereas the phase fronts (marked by red dot) move to the left [28].

choose the direction of energy flow as the reference propagation direction, the index of refraction must

be negative so that the wave vector $\vec{k}$ is in the opposite direction to the energy flow. For example, a Gaussian wave packet travels through the negative index material. Fig. 14 displays the propagation of a Gaussian wave packet in a negative-index material as time proceeds. The envelope of the packet propagates to the right, whereas the phase fronts (marked by red dot) move to the left.

5.2 EIT in Metamaterials

Electromagnetic induced transparency is a phenomena where an atomic medium becomes transparent over a very narrow frequency range to a probe field when a second strong pump beam is also present in the medium. EIT in atomic medium is thoroughly described in section 4. Recently, the analogue of EIT effect in metamaterial has attracted increasing attentions due to its advantages such as controllable room temperature and large operating bandwidth. The working principle of EIT metamaterial is based upon its unique structure. This material has two kinds of resonant structures, called as bright and dark resonators respectively. The bright resonator can directly couple with the incident EM wave but the dark resonator cannot. However the dark resonator can indirectly couple to the bright resonator. These two resonators have similar resonant frequency. When these two resonators are periodically arranged, EIT effect can be excited by near field couplings between two metamaterial based resonators.

In 2008, Zhang *et al.* [29] first proposed the concept of EIT metamaterial. As shown in figure 15(a), Zhang *et al.* designed and implemented the EIT metamaterial with a working frequency of 428.4 THz by taking a metallic short wire parallel to the incident electric field as a bright resonant unit and two metallic short wires perpendicular to the incident electric field as a dark resonant unit. The periodic array of EIT metamaterials is shown in figure 15(b). Here in EIT metamaterial, the interference between bright and dark resonant elements is determined by the separation d between them, rather than by the pump light, used in atomic system. The interference between the bright and dark resonant elements gives rise to a significant depression in the spectrum of the imaginary part of the E-field for all distances and the depth and width of the depression will also change with the different separation d figure (15 c), similar to EIT effects in the atomic coherent systems.

5.2.1 Categories of EIT metamaterials

Passive EIT metamaterials: Depending on the different operating frequency, EIT metamaterials can be divided into three categories

(a)Microwave EIT metamaterials

(b)Terahertz EIT metamaterials

(c)Plasmonic EIT metamaterials.

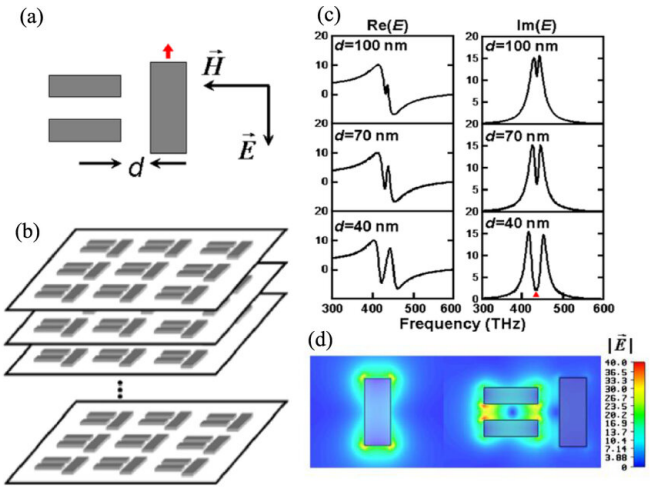

Figure 15: (a) unit cell configuration of EIT metamaterials, (b) periodic structure of EIT metamaterials, (c) plot of real and imaginary part of E field for differnt d, (d) E-field plots of bright structure. [29]

Active EIT metamaterials: One of the disadvantage of the passive EIT metamaterials is that once they are fabricated their properties are fixed which hinders the development and practical application of EIT. To overcome this difficulty the active EIT metamaterials are highly desirable. Till now many active materials have been incorporated to the construction of EIT metamaterials. Some of them are (a) graphene based EIT metamaterials and (b) photosensitive element based EIT metamaterials.

6 Surface plasmon polariton

SPPs are surface electromagnetic waves that propagate along the interface between a metal and a dielectric material and the surface electromagnetic waves consist of surface charges. We consider a p-polarized wave (TM mode, the electric field vector parallel to the incident plane) that reaches a smooth planar interface at an incident angle θ_1. The incident wave has a photon momentum $\hbar k_d$ ($k_d = \frac{2\pi n_d}{\lambda}$) in the dielectric with a refractive index n_d. When the wave arrives at the interface, the reflective wave will propagate along the direction with an angle equal to the incident angle and the photon momentum is conserved. Moreover, the wave in the metal propagates in a new direction with a refractive angle θ_2. The photon momentum is $\hbar k_m$ (where $k_m = \frac{2\pi n_m}{\lambda}$, n_m is the refractive index of the metal) and the momentum component along the x direction is conserved, i.e. $k_{dx} = k_{mx}$, where $k_{dx} = k_d \sin\theta_1$ and $k_{mx} = k_m \sin\theta_2$. In general, the refractive index of the dielectric n_d is larger than that of the metal n_m at the visible wavelength. Beyond the limiting angle, the wave cannot propagate in the metal. In this case, the limiting incident angle is called the critical angle θ_c, which is given by

$$sin\theta_c = \frac{n_m}{n_d} \tag{37}$$

For the p-polarized wave incident on the interface, the oscillating electric field will cause surface charges at the interface between the metal and the dielectric and the surface charges undergo a collective oscillation. Although the wave is totally reflected at the interface there are oscillating charges which have associated radiation fields penetrating into the metal. They are spatially decaying fields (evanescent fields) in a direction normal to the interface. At the critical angle the decay length is infinite but this falls rapidly to the order of the wavelength of light as the angle of incidence increases further. In these cases, the evanescent fields for the incident wave beyond the critical angle are useful for coupling radiation to SPPs.

6.1 EIT in SPR system

Recent theoretical investigation has shown that EIT can be used for coherent control of the group velocity of the polaritons at the surface of a negative refractive index metamaterial under the condition of near-zero loss of the polaritons. The EIT based coupler free SPR system comprises a top transparent medium (such as air or a thin vacuum), a middle metal thin film, and a dielectric bottom layer of a three-level atomic system. If the relative permittivity of the EIT atom becomes less than one, i.e., $\epsilon_d < 1$, then the wave number of SPPs becomes less than that of the incident light, i.e., $k_{spp} < k_0$. As a result, the resonance condition satisfies, i.e., $k_{spp} = k_0 \sin\theta$ and SPPs can be excited at a proper incident angle θ.

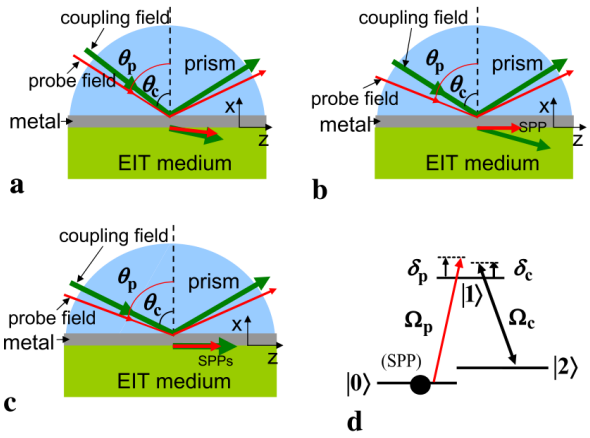

Figure 16: Schematic diagram of EIT based SPR [15]

Model and equation: We consider the case of freely propagating coupling field. The scheme of EIT-based SPR is shown in figure (16). The system is composed of an EIT medium (green), a metal film (gray) and a prism (blue). Here the EIT medium can be atomic gases or doped solid medium which are composed of three level atoms of Λ configuration, shown in figure (16 d).

In the case of $\theta_c < \theta_{crt}$, the coupling field in the dielectric is a freely propagating field (shown in figure (16a) and (16b)), and Ω_c is spatially independent. With effective-medium theory and taking

into account local field effects for generality, the permittivity of the atomic medium can be given by [30, 31]

$$\epsilon_d = \epsilon_b + \frac{\chi}{1-\frac{\chi}{3}}\frac{\epsilon_b+2}{3} \tag{38}$$

where ϵ_b is the background permittivity and χ ($\propto \rho$) is given by,

$$\chi = \frac{1}{2}\frac{|\mu_{10}|^2 N}{\hbar\epsilon_0} \times \frac{e^{i\phi}\frac{\Omega_m\Omega_c}{2} - (\Delta_p - \Delta_c + i\gamma/2)}{(\Delta_p - \Delta_c + i\gamma/2)(i\gamma/2 + \Delta_p) - |\frac{\Omega_c}{2}|^2} \tag{39}$$

The background is assumed to be a vacuum ($\epsilon_b = 1$) or a very dilute dielectric ($\epsilon_b \approx 1$). Here, N is the density of the atomic number. So, ϵ can be easily obtained with above equations, in particular, for dilute vapors ($\frac{1}{3}\chi << 1$), ϵ_d can be given by $\epsilon_d \approx \epsilon_b + \chi$.

It should be noted that, because the coupling field only drives transition between $|2\rangle$ and $|1\rangle$ of the atoms and the population in state $|2\rangle$ is near zero at all times, the effect of the atoms on the coupling field can be safely neglected. So, we only consider the effect of the atomic medium on the probe field. The reflectivity R of the probe beam defined by $R = |r_{pmd}|^2$, where r_{pmd} is the three-layer amplitude reflection coefficient and is given by the Fresnel formula

$$r_{pmd} = \frac{r_{pm} + r_{md}\exp\{(2ik_{mx}q)\}}{1 + r_{pm}r_{md}\exp\{(2ik_{mx}q)\}} \tag{40}$$

where q is the thickness of the metal film, and the two layer amplitude reflection coefficients r_{pm} and r_{md} at the prism/metal and metal/dielectric interfaces respectively and given by

$$r_{pm} = \frac{\epsilon_m k_{px} - \epsilon_p k_{mx}}{\epsilon_m k_{px} + \epsilon_p k_{mx}} \tag{41}$$

$$r_{md} = \frac{\epsilon_d k_{mx} - \epsilon_m k_{dx}}{\epsilon_d k_{mx} + \epsilon_m k_{dx}} \tag{42}$$

Here, k_z is parallel wave vector and can be given by

$$k_z = k_0 n_p \sin\theta_p \tag{43}$$

where $k_0 = \frac{\omega_p}{c}$ and k_{jx} are normal wave vectors and can be given by

$$k_{jx} = \sqrt{(k_0^2\epsilon_j - k_z^2)} \tag{44}$$

with $j = p, m, d$ denoting the prism, the metal and the dielectric (EIT medium) respectively. The field enhancement due to surface plasmon is defined by [32] $T = |t_{pmd}|^2$ with $t_{pmd} = \frac{H_y(\frac{m}{d})}{H_y(\frac{p}{m})}$, where $H_y(\frac{m}{d})$ and $H_y(\frac{p}{m})$ are the magnetic field at metal/dielectric and prism/metal interfaces respectively,

and t_{pmd} can be calculated with the Fresnel formula

$$t_{pmd} = \frac{t_{pmd}t_{md}\exp\{(ik_{mx}q)\}}{1 + r_{pm}r_{md}\exp\{(2ik_{mx}q)\}} \tag{45}$$

where $t_{ij} = 1+r_{ij}$ being derived from the boundary conditions, and $i, j = p, m$ or $i, j = m, d$. Similarly, we can also calculate the field enhancement of the electric field T_e, which is defined by

$$T_e = \frac{|E(\frac{m}{d})|^2}{|E(\frac{p}{m})|^2} \tag{46}$$

where $E(\frac{m}{d})$ and $E(\frac{p}{m})$ are the electric field at metal/dielectric and prism/metal interfaces respectively. For TM polarization, according to [32], the relation between T_e and T is given by $T_e = \frac{\epsilon_p}{\epsilon_d}T$. Using eq.(38) and (39) we can calculate the permittivity of the atomic medium and in combination with eq (40) to eq (44) we can calculate reflectivity (R) of the probe field laser beam.

7 Literature Survey

7.1 Experimental Understandings

7.1.1 Experimental Observation

1976: G.Alzetta *et al.* were the first to experimentally observe the quantum coherence phenomenon known as Coherent Population Trapping (CPT) [2]. During their investigation of magnetic resonance, they observed three black lines in the fluorescence of sodium atoms along the path of the laser beam.

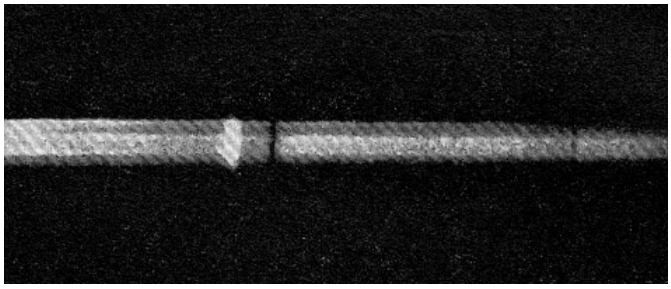

Figure 17: First observation of Coherent Population Trapping [2]

1976-1990: In 1976, Arimondo [3] conducted a theoretical analysis considering coherence phenomena in a three-level system. This analysis was based on the solution of the Bloch equation for a three-level system in a folded configuration. Two years later, Gray [25] independently observed similar behaviour. Following the theoretical work on optical coherence in 1976, Bright reviewed the use of electromagnetic fields to create transparency in 1984. In 1986, Kocharovskaya and Khanin's [33] theoretical work with the Λ configuration predicted population trapping in two lower levels. The

foundations of EIT were laid by Kocharovskaya and Khanin in 1988 and independently by Harris in 1989 [4].

1990: The name EIT was first proposed by Harris [26]. In their paper, they proposed the resonantly enhanced non-linear susceptibility based on EIT. The first experimental demonstration of EIT was also done by the Harris Group in 1991[27]. This experiment, conducted in a Λ scheme in strontium vapor using pulsed lasers, showed that the transmittance of the probe field coupling a lower lying state and an upper state could be increased from e^{-20} (without the coupling field) to e^{-1} (with the coupling field). The authors emphasized the significance of quantum interference in this enhancement, noting that without interference, the transmittance would have only increased to e^{-7}.

1991-1998: Field *et al.* [34] provided the first observation of EIT in a collision-broadened resonance transition of lead (Pb) vapor and anticipated its application to nonlinear optical processes. Scully [35] was the first to show that, it is possible to achieve a significant enhancement of the refractive index through quantum interference and coherence. Following the strontium experiment, Kasapi demonstrated EIT in a cascade (Ξ) scheme in lead vapor in [36]. Eberly and his group first observed the spatial evolution of dressed field pulses, analogous to the temporal evolution of dressed atoms, providing crucial information on EIT propagation. Fulton *et al.* [37] conducted theoretical and experimental investigations into the viability of Λ, Ξ and V type systems within rubidium (Rb) atoms for the observation of EIT. In 1996, Kasapi [36] applied EIT to isotope discrimination by adjusting the intensity of a coupling laser, rendering one isotope resonantly opaque while making another transparent to a probe. Hopkins *et al.* [38] investigated EIT in a laser-cooled medium in a magneto-optical trap, examining Λ-type configurations of hyperfine levels of the D_2 line and systems utilizing degenerate Zeeman sublevels of the ground state. Azim *et al.* [39] proposed a method to measure photon statistics of a quantized radiation field in an EIT setup. Boon and his group [40] presented an experimental observation of transparency in the blue spectral region, induced by a continuous wave infrared coupling field in a Doppler-broadened medium. This experimental result, using a V-type scheme in atomic rubidium vapor, was supported by extensive theoretical modeling of the system.

1999: Danish physicist Lene Vestergaard Hau [10] led combined team from Harvard University and the Rowland Institute for Science reported an experimental demonstration of EIT in an ultra cold gas of sodium atoms, where optical pulses propagated at speeds twenty million times slower than the speed of light in a vacuum. The gas was cooled to nano kelvin temperatures using laser and evaporative cooling system. Quantum interference, which controlled the optical properties of the medium, was established by a coupling laser beam propagating at a right angle to the pulsed probe beam. With the high atomic density, they succeeded in slowing a beam of light to approximately 17 meters per second using the EIT technique.

7.1.2 Further experimental advancements

1. **EIT in different three level systems:** Entin *et al.* [41] experimentally demonstrated non degenerate four-level N-type scheme to observe EIT at the ^{87}Rb D_2 line. Then Badger with his co workers [42] investigated the role of hyperfine structure in EIT by studying the $5S_{1/2}$–$5P_{3/2}$–$5D_{3/2,5/2}$ cascade system in ^{85}Rb and ^{87}Rb. Chen *et al.* [43] first reported an experimental observation of narrow and high-contrast spectra, induced by interacting dark resonances in a three-level Λ-type configuration. Then Min Yan and his group [44] reported experimental studies of EIT in Λ-type and ladder (Ξ) type atomic systems in 87_{Rb} atoms, cooled and confined in a magneto-optical trap. The Λ-type system with a moderate coupling field shows complete transparency. Wang and his co workers [45] reported an experimental investigation of EIT in a multi-level cascade system of cold ^{85}Rb atoms. In 2005, Chakrabarti *et al.* [46] showed that the pump-probe spectroscopy of Λ-type system for the D_2 transition of ^{87}Rb exhibits additional absorption enhancement peaks due to velocity selective optical pumping along with EIT. The separation of those peaks were consistent with the hyperfine splitting of the upper levels. For ^{85}Rb, peaks were not clearly seen since the hyperfine splitting were much smaller. Li *et al.* [47] in 2009 worked on realization of a single and closed Λ-system in a room temperature three-level coherently prepared resonant medium with narrow D_1 hyperfine splittings. The coherent pump–probe spectroscopy of a Λ system with a closely lying excited level was investigated by singh *et al.*[48].

2. **Dispersive properties of EIT:** In 2001, Dogariu *et al.* [49] demonstrated both theoretically and experimentally that transparent linear anomalous dispersion can occur in the presence of a gain doublet. They predicted that superluminal light-pulse propagation could be observed even at a negative group velocity through a transparent medium with almost no pulse distortion. Later, Kim *et al.* [50] and Gang *et al.* [51] conducted further experimental work in this field.

3. **EIT in cavity:** Opatrny *et al.* [52] proposed an optical double cavity resonator with a response to signals similar to that of an EIT medium. Mucke *et al.*, Genes *et al.*, and Han *et al.* investigated EIT with atoms in a cavity [53, 54, 55]. Recently, Khoa *et al.* [56] measured the dispersive profile of a multi-window EIT spectrum in a Doppler broadened atomic medium.

4. **Kerr nonlinearity:** In 2001, Wang *et al.* [57] measured the Kerr nonlinear index of refraction in a three-level Λ-type atomic system within an optical ring cavity. They observed that the Kerr nonlinearity was significantly modified and enhanced near atomic resonance conditions for both probe and coupling beams. Akulshin *et al.* [58] demonstrated that long-lived bright Zeeman coherence, which is responsible for absorption enhancement and steep anomalous dispersion in an atomic medium, leads to a high nonlinearity in atomic susceptibility. Kang *et al.* [59] reported

the experimental observation of large Kerr nonlinearity with vanishing linear susceptibilities in coherently prepared four-level rubidium atoms. Kou *et al.* [60] investigated EIT-assisted large cross-kerr nonlinearity in a four level inverted Y atomic system.

5. **Two photon transparency:** Wang *et al.* [57] experimentally demonstrated electromagnetically induced two photon transparency in room temperature Rb vapour. In 2006, Jiang *et al.* [61] observed the two-photon absorption in a four level system in hot ^{87}Rb vapour. They showed that this effect can be reduced in hot atoms due to the non Doppler free nature of this scheme.

6. **Group velocity reduction and light storage:** In 2002, several researchers reported significant advancements in optical pulse manipulation. Kozuma *et al.* [62] explored optical pulse group velocity reduction and regeneration using a Raman scheme, which has advantages over traditional EIT methods. Mair *et al.* [63] demonstrated phase coherence and control in light storage. Petrosyan *et al.* [64] proposed a scheme for efficient nonlinear interactions between weak optical fields via EIT. Bajcsy *et al.* [65] showcased a technique to convert light into localized stationary electromagnetic energy in Rb atoms, allowing controlled release and manipulation of photon states. Figueroa *et al.* [66] studied squeezed vacuum transmission and storage under EIT in Rubidium, while Phillips *et al.* [67] performed experimental light storage in an optically thick atomic ensemble using EIT and four wave mixing.

7. **Works on width of EIT resonance and line shape:** Several studies have investigated the temporal evolutions and characteristics of EIT and EIA in various atomic systems. Valente *et al.* [68] observed these phenomena in ^{87}Rb vapor during Hanle absorption experiments by toggling the magnetic field. Alzar *et al.* [69] measured intensity fluctuations of beams interacting with Rb atoms in EIT conditions in 2003. Feng [70] detected EIT in a Rubidium vapor system at 348K with a 0.6 MHz signal width. Alzetta *et al.* [71] achieved complete EIT in Sodium vapor using a broadband dye laser on the D1 line in 2004. Carvalho's team [72] studied the linewidth dependence of EIT resonance on beam angles in Cesium vapor, noting significant broadening due to non parallel beams. Krishna *et al.* [73] explored high resolution hyperfine spectroscopy using EIT, while Sautenkov, Xiang [74, 75] and others investigated EIT resonance widths for applications in magnetometry, atomic clocks and frequency chains. Cuk *et al.* [76] examined how laser beam intensity distribution affects Zeeman EIT line shapes in vacuum Rb cells.

8. **Further experimental works:** Wei *et al.* [77] studied EIT in ^{87}Rb vapor at 325 K, confirming that EIT sub-windows depend on magnetic field orientation. Wen *et al.* [78] examined the generation of entangled photon pairs in an EIT system, focusing on transverse effects and phase matching conditions using quantum theory. Kang *et al.* [59] measured resonant four-wave mixing in cold Rb atoms. Bell and Abel [79, 80] worked on laser frequency offset locking using EIT.

In 2010, Krmpot *et al.* [81] studied optical pumping spectroscopy with co-propagating laser beams in Rb vapor. Pandey *et al.* [82] showed EIT splitting under strong-probe conditions due to Doppler averaging. Reshetov *et al.* [83] conducted EIT experiments with degenerate atomic levels. Bhattacharyya *et al.* [84] observed EIT in a six level Λ-type system in Rb vapor. Kalatskiy *et al.* [85] worked on frequency stabilization of a diode laser for the 5P → 5D transition of Rb atoms in 2017. In 2018, Yadav *et al.* [86] explored five and seven level inhomogeneously broadened Ξ type systems with mismatched wavelengths and polarization effects.

7.2 Theoretical Understandings

7.2.1 Density matrix formalism

1. **EIT in different types of systems:**

   (a) **Λ type system:** Rathe *et al.* and Hansch *et al.* [87] explored the nonlinear electric susceptibility behavior in several high refractive index systems without absorption, attributed to quantum coherence and interference. Matsko *et al.* [88] demonstrated that adiabatic passage is unnecessary for information storage and retrieval in optically thick vapor of Λ-type atoms. Chakrabarti *et al.* [46] investigated velocity selective optical pumping effects and EIT for D2 transitions in Rb atom. Geller *et al.* [89] in 2007 examined the influence of atomic thermal motion on EIT manifestations in gaseous media. Brzostowski *et al.* [90] theoretically developed EIT in a Four-Level Λ scheme of cold Rb atoms. Mishina *et al.* [91] focused on enhancing EIT in room temperature alkali metal vapor. He *et al.* [92] investigated coherent hole-burnings induced by a bichromatic laser field. Yang *et al.* [93] reported on the influence of EIT effect with double windows on electromagnetic characteristics of quasi Λ four-level atomic systems. Raheli *et al.* [94] performed atom position measurements in a four-level Λ shaped scheme with two lower-levels.

   (b) **Ξ type system:** Banacloche and his co-workers [95] in University of Arkansas developed a theory of EIT in three level ladder type Doppler broadened medium. Ling *et al.* [96] demonstrated that a strong coupling standing wave can diffract a weak probe field as a grating with Ξ or ladder-type atoms. McGloin *et al.* [97] explored EIT in a Ξ type system with N levels and N-1 fields. Dutta *et al.* [98] investigated nonlinear optical effects in a doubly driven four-level atom. Khoa *et al.* [56] analytically demonstrated EIT in a five-level cascade system under Doppler broadening. Hamedi *et al.* [99] reported high refractive index and lasing without inversion in an open four level atomic system. Kumar *et al.* [100] presented a theory of EIT and slow light in a Doppler broadened three-level ladder system, considering residual Doppler broadening of two photon coherence.

   (c) **Vee type system:** Lee *et al.* [101], Dutta *et al.* [102], Han *et al.* [103] theoretically

demonstrated EIT and lasing in a Vee-type system without population inversion. Hu *et al.* [104] provided a theoretical analysis of the spectral linewidth of the Vee-type system. Dey *et al.* [105], Hoshina *et al.* [106] investigated EIT in a multi V type system. Mousavi *et al.* [107] reported the effect of quantum interference on the optical properties of a three-level V-type atomic system beyond the two photon resonance condition.

(d) **Inverted Y type system:** Yan *et al.*[108] explored EIT in an inverted-Y system of interacting cold atoms. Osman *et al.* [109] investigated the effect of spontaneously generated coherence on EIT and its refractive properties in four and five-level systems. Kou *et al.* [110] delved into EIT and its dispersion properties in a four-level inverted Y atomic system. Liu *et al.* [47] reported on ultra-slow soliton pairs in a four level inverted Y system via EIT. Ghosh *et al.* [111] observed the occurrence of EIT in the simulated probe response signal for a four level inverted Y type system under the influence of a weak coherent probe field, a strong coherent pump field, and a coherent pump field.

(e) N **level system and Rydberg EIT:** In 2008, Anton *et al.* [112] delved into optical switching in a five level atom through EIT. Chen *et al.* [113] and Kong *et al.* [114] explored the optical properties of an N-type system in Doppler broadened multilevel atomic media. Wu *et al.* [115] reported eight wave mixing via EIT. Golubev *et al.* [116] theoretically modeled the control of group velocity of light through a magnetic field. Naber *et al.* [117] investigated EIT with Rydberg atoms across the Breit-Rabi regime. Tian *et al.* [118] modeled EIT in a Y system with a single Rydberg state. Kara *et al.* [119] studied Rydberg interaction induced enhanced excitation in thermal atomic vapor.

7.2.2 Other approaches

Silva *et al.*[5] investigated EIT in closed Doppler broadened three level systems, where a probe traveling wave laser field interacted with a standing wave laser field of moderate intensity. A method proposed by A. Imamoglu aims to achieve nearly ideal photon counting through a combination of photonic quantum memory and ion trap quantum state measurements. Kuang *et al.* [120] presented a method for generating continuous variable type entangled states between photons and atoms in atomic Bose-Einstein condensates. Beausoleil *et al.* [121] outlined the requirements for components in the Quantum Information Technology (QIT) industry, emphasizing EIT's potential role in enabling few-qubit quantum information processing. Jing *et al.* [122] proposed a scheme for quantum state storage and manipulation using EIT in flexible multi ensemble systems of three-level atoms. Sun *et al.* [123] focused on optical beam steering through electromagnetically induced transparency. Kumar *et al.* [100] studied EIT in multi level cascaded type system in cold atoms using an optical nanofiber interface.

7.3 Metamaterials:

7.3.1 Theoretical concept (1968)

V.G.Veselago [13] first theorized the behavior of materials with simultaneously negative values of the electric permittivity ϵ and magnetic permeability μ. He showed that in this case, the solution of the Maxwell equations resulted in an index of refraction with a negative real part. In such materials, the vectors $\vec{E}$, $\vec{H}$ and $\vec{k}$ (the electric field, magnetic field and wave vectors respectively) would form a left-handed set and the phase velocity is thus opposite to the energy flux. This would cause negative refraction at the boundary between two media with opposite signs of n.

7.3.2 Experimental demonstration of NIM (Early to Mid 2000s)

1. **In 1999**, Sir John Pendry [14, 124] first shows the path for developing NIM. He pointed out that sub-wavelength metalic resonant structures called split ring resonator (SSR) would exhibit negative μ at specific frequencies.

2. **2000-2001:** Smith *et al.* [125] demonstrated the first metamaterial with a negative refractive index at microwave frequencies using split-ring resonators (SRRs) and wire structures. Shelby *et al.* [125] demonstrated negative refraction using a metamaterial wedge. In both cases SSR's operating in Gigahertz domain.

3. **2003-2005:** During this period the main focus of the researchers was to achieve negative μ at higher frequency so that the material can operate in optical frequency region. Scaling down the size of SSR leads to a response at higher frequency. The resonance frequency has been pushed up to 1 THz using this scaling technique by Yen *et al.*[126]. Zhang *et al.* [127, 128] gave an alternative to double SRRs which enables the resonance frequency to be shifted to 60 THz. As demonstrated by Linden and co-workers [129], single SRRs that show an electric response at 85 THz can also provide a magnetic response at this frequency range. The development of negative refractive index materials (NRIM), also known as metamaterials, has seen significant advancements since 2005. These materials, which have a refractive index that is negative for certain wavelengths, have unique properties allowing them to manipulate electromagnetic waves in ways that natural materials cannot. Here is a summary of the key advancements in NRIM from 2005 onwards:

4. **2005-2010: Early development and demonstrations** In the year 2007, Shaleav *et al.*[130, 131] highlighted early experimental demonstrations of optical NIMs, discussing various designs and materials used to achieve negative refractive indices at optical frequencies. The study provided a comprehensive overview of the theoretical underpinnings and initial experimental results. In the same year Soukoulis *et al.* [132] reviewed the progress in achieving negative

refractive index materials at optical wavelengths. The focus was on the design principles, such as the use of split-ring resonators (SRRs) and fishnet structures[133, 134].

5. **2010-2015: Expansion and Optimization**

   Broadband metamaterials: Development of broadband negative refractive index materials, which work across a wider range of wavelengths, was achieved during this time. This involved creating structures with multiple resonant elements or using tunable materials [135, 136].

   Three-dimensional metamaterials: Advancements were made in creating three dimensional negative refractive index materials, as opposed to the earlier two dimensional designs. This expanded the potential applications and efficiency of these materials [137].

6. **2015-2020: Further Advancement**

   Quantum metamaterials: The integration of metamaterials with quantum dots and other quantum systems to create quantum metamaterials was explored. These materials could potentially interact with quantum light fields, leading to advances in quantum computing and communications [138, 139].

   Active metamaterials: Development of active metamaterials that can change their properties dynamically in response to external stimuli, such as electric or magnetic fields, allowed for the creation of tunable and reconfigurable devices [140, 141].

7. **2020 and beyond: Emerging trends**

   Topological photonics: Research into topological insulators inspired new types of metamaterials that are robust against defects and can support unique modes of light propagation, promising advancements in optical communications and computing.

   Biological metamaterials: The intersection of metamaterials and biotechnology opened new avenues for biosensing and medical diagnostics, using the unique properties of negative refractive index materials to detect biological molecules with high sensitivity.

   Environmental sensing and energy harvesting: Metamaterials are being explored for environmental sensing applications and energy harvesting, including improved solar cells and sensors capable of detecting pollutants at very low concentrations.

The advancements in negative refractive index materials since 2005 have not only expanded our understanding of electromagnetic wave manipulation but also paved the way for numerous innovative applications in various fields, from imaging and telecommunications to quantum technologies and beyond.

7.3.3 EIT metamaterial

1. **First experimental demonstration:** EIT in metamaterials was first shown by Zhang *et al.* in **2008** [29]. He designed and implemented the EIT metamaterial with a working frequency of 428.4 THz. Since Zhang *et al.* proposed the concept of EIT metamaterial, EIT effect analogs in metamaterials have received a growing number of attentions from microwave to optical frequencies.

2. **EIT in THz domain and plasmonic EIT (2009):** In 2009, Sher-Yi Chiam et. al. [142, 143] have experimentally demonstrated EIT using THz time domain spectroscopy (THz-TDS). They studied the mimicking EIT like phenomenon by using a planar metamaterial composed of SRRs and close rings. Researchers developed plasmonic EIT structures, which used plasmonic resonances in metallic nanostructures to achieve transparency effects similar to atomic EIT. Liu *et al.* (2009) [144] showed EIT in planar metamaterials with a sharp transmission peak, paving the way for practical applications.

3. **Further advanced techniques (2015-2020) :** Since 2010, significant progress has been made in the field of EIT in metamaterials, from foundational studies and initial demonstrations to advanced designs and practical applications. Researchers have explored various materials, including metals, graphene and hybrid systems to achieve tunable and reconfigurable EIT effects.

   In year 2018, Ling *et al.* [96] numerically demonstrated a plasmonic metamaterial that can realize controllable EIT effect via polarization selection and its unit cell is constituted of perpendicular gold bar pairs system, which is an ideal platform to generate EIT effect with strong dispersion. In this era , a lot of microstructures and methods to realize PIT effects have been proposed. As long as the polarization state of incident E-field is changed, the number of transparent windows can be controlled, which possesses the advantages of adjustable amplitude and resonance wavelength. In 2020, Tang *et al.* [145] proposed a three-band EIT metamaterial consisting of two nested π-type metallic structures.

4. **2020 Onwards:** Xiao *et al.* [146] in 2020 designed a metasurface structure based on graphene that exhibited a tunable EIT response in the near infrared bands. They demonstrated that the resonant frequency of EIT effect can be dynamically manipulated by regulating the external voltage so as to adjust the Fermi level of graphene. Zhou *et al.* [147] imported Ge and Si as

active materials into the EIT metamaterial. Like this several advance techniques have been adopted for development of EIT effect in metamaterial.

7.4 EIT-based Surface Plasmon Polariton :

In 1997, Barren *et al.* [148] studied the propagation of surface plasmon polaritons on textured surfaces, specifically on a grating surface.

In 1998, a method is reported for exciting surface plasmon polaritons with a focused laser beam as the excitation probe by Kano *et al.* [149]. They calculated the electric field intensity distribution on a silver surface which is caused by the excited surface plasmon polaritons. In the same year, elastic scattering of surface plasmon polaritons (SPP's) was first modeled by Bozhevolnyi *et al.* [150] by considering isotropic point like scatterers whose responses to the incident SPP field are phenomenologically related to their effective polarizabilities.

In 2002, Ditlbacher *et al.* [151] reported the experimental realization of highly efficient optical elements built up from metal nanostructures to manipulate surface plasmon polaritons propagating along a polymer interface.

Near field imaging of scattering, reflection, interference and localization of surface polaritons are reviewed by Zayats and Smolyaninov [152] in **2003**.

In 2004, Krenn and Weeber [153] investigated SPP properties such as propagation length, mode field profile and reflection or scattering at metal dielectric interfaces. Various techniques for SPP excitation and detection are discussed in their paper.

In 2005, Andre *et al.* [154] presented an overview of recent theoretical and experimental work on the control of the propagation and quantum properties of light using electromagnetically induced transparency in atomic ensembles. They provided the techniques for the generation and storage of few photon quantum-mechanical states of light as well as novel approaches to manipulate weak pulses of light via enhanced nonlinear optical processes.

In 2010, Lu *et al.* [155] showed that magnetic plasmon resonance play a vital role in plasmonic electromagnetically induced transparency (EIT). Their interaction was investigated in detail by analyzing the phase evolution of the induced electromagnetic fields in nanoscale volume, which is rendered by the unique near-field properties.

Chen *et al.* [156] in **2011**, have explored a coupling system structure consisting of cross-slit metallic photonic crystals and dielectric photonic crystals embedded in a background material to achieve polarization independent plasmon induced transparency.

In 2015, Du *et al.*[157] first proposed a way to excite SPPs resonantly by lights without using any coupler and a surface-plasmon-resonance (SPR) system which can be simply composed by a metal film and a bottom medium whose real part of permittivity is less than unity. In the same year Meng *et al.* [158] theoretically studied EIT in reflection spectra of V-type system at the gas-solid interface.

In addition to finding a narrow dip arising from the EIT effect, they also explored the other particular saturation effect induced by pump field, which does not exist in Λ or Ξ -type system.

Asgarnezhad *et al.* [159] in **2017** investigated the possibility of the direct excitation of surface polaritons (SPs) by the free-space laser fields at the interface of negative-index metamaterial (NIMM) layer and a bottom layer of cold double Λ-type atomic medium. The giant field enhancement together with suppressed ohmic loss of the NIMM layer in a wide transparency window of a double EIT, results in the SPs generation.

In the following year, the same group [160] investigated the excitation and propagation of the surface polaritonic rogue waves by proposing a coupler free optical waveguide that consists of a transparent layer, middle negative index metamaterial layer, and bottom layer of the cold four level atomic medium. In this planar optical waveguide, a giant controllable Kerr nonlinearity is achieved by sufficient field concentration and a proper set of intensities and detunings of the driven laser fields.

8 Future outlook

After the completion of detailed study of the coherent optical phenomena (*e.g.,* EIT, EIA, AT dips) in both the gaseous and solid mediums, we shall design both the different atom-laser coupled systems and SPP-laser coupled systems. The theoretical modelling of the interaction of such systems will be presented in detail to study the coherent optical responses. We shall also focus on a thorough study of surface plasmon polariton to investigate a similar kind of optical response at metal-dielectric interface from the reflected probe beam. Moreover, we shall explore the probe beam's optical responses by controlling the different degrees of freedom of laser lights.

References

[1] Claude Cohen-Tannoudji, Jacques Dupont-Roc, and Gilbert Grynberg. *Atom-photon interactions: basic processes and applications*. John Wiley & Sons, 1998.

[2] GAML Alzetta, A Gozzini, L Moi, G Orriols, et al. An experimental method for the observation of rf transitions and laser beat resonances in oriented na vapour. *Nuovo Cimento B*, 36(5), 1976.

[3] EetGORRIOLS Arimondo and G Orriols. Nonabsorbing atomic coherences by coherent two-photon transitions in a three-level optical pumping. *Nuovo Cimento Lettere*, 17:333–338, 1976.

[4] Stephen E Harris. Lasers without inversion: Interference of lifetime-broadened resonances. *Physical review letters*, 62(9):1033, 1989.

[5] F Silva, J Mompart, Verònica Ahufinger, and R Corbalan. Electromagnetically induced transparency with a standing-wave drive in the frequency up-conversion regime. *Physical Review A*, 64(3):033802, 2001.

[6] Marlan O Scully, Shi-Yao Zhu, and Athanasios Gavrielides. Degenerate quantum-beat laser: Lasing without inversion and inversion without lasing. *Physical review letters*, 62(24):2813, 1989.

[7] U Fano. Nuova cimenta 12, 156 (1935). *Phys. Rev*, 124:1886, 1961.

[8] Paul Forman. Atomichron®: the atomic clock from concept to commercial product. *Proceedings of the IEEE*, 73(7):1181–1204, 1985.

[9] David F Phillips, Anett Fleischhauer, A Mair, Ronald L Walsworth, and Mikhail D Lukin. Storage of light in atomic vapor. *Physical review letters*, 86(5):783, 2001.

[10] Lene Vestergaard Hau, Stephen E Harris, Zachary Dutton, and Cyrus H Behroozi. Light speed reduction to 17 metres per second in an ultracold atomic gas. *Nature*, 397(6720):594–598, 1999.

[11] Olga Kocharovskaya. Amplification and lasing without inversion. *Physics Reports*, 219(3-6):175–190, 1992.

[12] Pradip K Ghosh. *Ion traps*. Oxford university press, 1995.

[13] Viktor G Veselago. Electrodynamics of substances with simultaneously negative and. *Usp. fiz. nauk*, 92(7):517, 1967.

[14] John Brian Pendry. Negative refraction makes a perfect lens. *Physical review letters*, 85(18):3966, 2000.

[15] Chunguang Du. Quantum surface plasmon resonance system based on electromagnetically induced transparency. *Applied Physics A*, 109:797–803, 2012.

[16] Robert Williams Wood. Xlii. on a remarkable case of uneven distribution of light in a diffraction grating spectrum. *The London, Edinburgh, and Dublin Philosophical Magazine and Journal of Science*, 4(21):396–402, 1902.

[17] William L Barnes, Alain Dereux, and Thomas W Ebbesen. Surface plasmon subwavelength optics. *nature*, 424(6950):824–830, 2003.

[18] G Raschke, S Brogl, AS Susha, AL Rogach, TA Klar, J Feldmann, B Fieres, N Petkov, T Bein, A Nichtl, et al. Gold nanoshells improve single nanoparticle molecular sensors. *Nano letters*, 4(10):1853–1857, 2004.

[19] Jiří Homola. Present and future of surface plasmon resonance biosensors. *Analytical and bioanalytical chemistry*, 377:528–539, 2003.

[20] Kazuo Tanaka and Masahiro Tanaka. Simulations of nanometric optical circuits based on surface plasmon polariton gap waveguide. *Applied Physics Letters*, 82(8):1158–1160, 2003.

[21] Th W Hansch, IS Shahin, Schawlow, and AL. High-resolution saturation spectroscopy of the sodium d lines with a pulsed tunable dye laser. *Physical Review Letters*, 27(11):707, 1971.

[22] Alan Corney. *Atomic and laser spectroscopy*. Clarendon Press Oxford, 1978.

[23] Pradip Narayan Ghosh. *Laser Physics and Spectroscopy*. CRC Press, 2018.

[24] Pierre Meystre and Murray Sargent. *Elements of quantum optics*. Springer Science & Business Media, 2007.

[25] HR Gray, RM Whitley, and CR Stroud. Coherent trapping of atomic populations. *Optics letters*, 3(6):218–220, 1978.

[26] Stephen E Harris, JE Field, and A Imamoğlu. Nonlinear optical processes using electromagnetically induced transparency. *Physical Review Letters*, 64(10):1107, 1990.

[27] K-J Boller, A Imamoğlu, and Stephen E Harris. Observation of electromagnetically induced transparency. *Physical Review Letters*, 66(20):2593, 1991.

[28] Wounjhang Park and Jinsang Kim. Negative-index materials: Optics by design. *MRS bulletin*, 33(10):907–914, 2008.

[29] Shuang Zhang, Dentcho A Genov, Yuan Wang, Ming Liu, and Xiang Zhang. Plasmon-induced transparency in metamaterials. *Physical review letters*, 101(4):047401, 2008.

[30] DE Aspnes. Local-field effects and effective-medium theory: a microscopic perspective. *American Journal of Physics*, 50(8):704–709, 1982.

[31] Michael E Crenshaw and Charles M Bowden. Local-field effects in a dense collection of two-level atoms embedded in a dielectric medium: intrinsic optical bistability enhancement and local cooperative effects. *Physical Review A*, 53(2):1139, 1996.

[32] Heinz Faether. Surface plasmons. *Smooth and Rough Surfaces and on Gratings (Springer Tracts in Modem Physics 111*, pages 642–646, 1988.

[33] A Kocharovskaya and Ya I Khanin. Population trapping and coherent bleaching of a three-level medium by a periodic train of ultrashort pulses. *Zh. Eksp. Teor. Fiz*, 90:1610–1618, 1986.

[34] JE Field, KH Hahn, and SE Harris. Observation of electromagnetically induced transparency in collisionally broadened lead vapor. *Physical review letters*, 67(22):3062, 1991.

[35] Marlan O Scully. Enhancement of the index of refraction via quantum coherence. *Physical Review Letters*, 67(14):1855, 1991.

[36] A Kasapi. Enhanced isotope discrimination using electromagnetically induced transparency. *Physical review letters*, 77(6):1035, 1996.

[37] David J Fulton, Sara Shepherd, Richard R Moseley, Bruce D Sinclair, and Malcolm H Dunn. Continuous-wave electromagnetically induced transparency: a comparison of v, λ, and cascade systems. *Physical Review A*, 52(3):2302, 1995.

[38] SA Hopkins, E Usadi, HX Chen, and AV Durrant. Electromagnetically induced transparency of laser-cooled rubidium atoms in three-level λ-type systems. *Optics communications*, 138(1-3):185–192, 1997.

[39] Tasnim Azim and M Suhail Zubairy. Measurement of photon statistics via electromagnetically induced transparency. *Physics Letters A*, 250(4-6):344–348, 1998.

[40] JR Boon, E Zekou, DJ Fulton, and MH Dunn. Experimental observation of a coherently induced transparency on a blue probe in a doppler-broadened mismatched v-type system. *Physical Review A*, 57(2):1323, 1998.

[41] VM Entin, II Ryabtsev, AE Boguslavskii, and IM Beterov. Experimental implementation of a four-level n-type scheme for the observation of electromagnetically induced transparency. *Journal of Experimental and Theoretical Physics Letters*, 71:175–177, 2000.

[42] SD Badger, IG Hughes, and CS Adams. Hyperfine effects in electromagnetically induced transparency. *Journal of Physics B: Atomic, Molecular and Optical Physics*, 34(22):L749, 2001.

[43] Ying-Cheng Chen, Yean-An Liao, Hsin-Ying Chiu, Jung-Jung Su, and A Yu Ite. Observation of the quantum interference phenomenon induced by interacting dark resonances. *Physical Review A*, 64(5):053806, 2001.

[44] Min Yan, Edward G Rickey, and Yifu Zhu. Electromagnetically induced transparency in cold rubidium atoms. *JOSA B*, 18(8):1057–1062, 2001.

[45] J Wang, LB Kong, XH Tu, KJ Jiang, K Li, HW Xiong, Yifu Zhu, and MS Zhan. Electromagnetically induced transparency in multi-level cascade scheme of cold rubidium atoms. *Physics Letters A*, 328(6):437–443, 2004.

[46] Shrabana Chakrabarti, Amitkiran Pradhan, Biswajit Ray, and Pradip N Ghosh. Velocity selective optical pumping effects and electromagnetically induced transparency for d2 transitions in rubidium. *Journal of Physics B: Atomic, Molecular and Optical Physics*, 38(23):4321, 2005.

[47] Ke Li, Lu Deng, and MG Payne. Realization of a single and closed λ-system in a room-temperature three-level coherently prepared resonant medium with narrow d1 hyperfine splittings. *Applied Physics Letters*, 95(22), 2009.

[48] Niharika Singh, Ayan Ray, R D'Souza, QV Lawande, and BN Jagatap. Coherent pump–probe spectroscopy of a λ system with a close lying excited level. *Physica Scripta*, 88(6):065404, 2013.

[49] A Dogariu, A Kuzmich, and LJ Wang. Transparent anomalous dispersion and superluminal light-pulse propagation at a negative group velocity. *Physical Review A*, 63(5):053806, 2001.

[50] Kyoung-Dae Kim, Mi-Rang Kwon, Jung-Bog Kim, and Han-Seb Moon. Observation of the electromagnetically induced transparency and dispersion-like structure in trapped cs atoms. *Journal of the Optical Society of Korea*, 5(4):131–135, 2001.

[51] Xiao-Gang Lu, Xing-Xu Miao, Jin-Hai Bai, Yuan Yuan, Ling-An Wu, Pan-Ming Fu, Ru-Quan Wang, and Zhan-Chun Zuo. Crossover between electromagnetically induced transparency and autler–townes splitting with dispersion. *Chinese Physics B*, 24(9):094204, 2015.

[52] T Opatrnỳ and D-G Welsch. Coupled cavities for enhancing the cross-phase-modulation in electromagnetically induced transparency. *Physical Review A*, 64(2):023805, 2001.

[53] Martin Mücke, Eden Figueroa, Joerg Bochmann, Carolin Hahn, Karim Murr, Stephan Ritter, Celso J Villas-Boas, and Gerhard Rempe. Electromagnetically induced transparency with single atoms in a cavity. *Nature*, 465(7299):755–758, 2010.

[54] Claudiu Genes, Helmut Ritsch, Michael Drewsen, and Aurélien Dantan. Atom-membrane cooling and entanglement using cavity electromagnetically induced transparency. *Physical Review A*, 84(5):051801, 2011.

[55] Yan Han, Jiong Cheng, and Ling Zhou. Electromagnetically induced transparency in a cavity optomechanical system with an atomic medium. *Journal of Physics B: Atomic, Molecular and Optical Physics*, 44(16):165505, 2011.

[56] Dinh Xuan Khoa, Pham Van Trong, Nguyen Huy Bang, et al. Electromagnetically induced transparency in a five-level cascade system under doppler broadening: an analytical approach. *Physica Scripta*, 91(3):035401, 2016.

[57] Lij // ijun J Wang, A Kuzmich, and Arthur Dogariu. Gain-assisted superluminal light propagation. *Nature*, 406(6793):277–279, 2000.

[58] Alexander M Akulshin, Andrei I Sidorov, Russell J McLean, and Peter Hannaford. Enhanced atomic kerr nonlinearity in bright coherent states. *Journal of Optics B: Quantum and Semiclassical Optics*, 6(12):491, 2004.

[59] Hoonsoo Kang and Yifu Zhu. Observation of large kerr nonlinearity at low light intensities. *Physical review letters*, 91(9):093601, 2003.

[60] Jun Kou, RG Wan, ZH Kang, HH Wang, L Jiang, XJ Zhang, Y Jiang, and JY Gao. Eit-assisted large cross-kerr nonlinearity in a four-level inverted-y atomic system. *JOSA B*, 27(10):2035–2039, 2010.

[61] Wei Jiang, Qun-feng Chen, Yong-sheng Zhang, and G-C Guo. Optical pumping-assisted electromagnetically induced transparency. *Physical Review A*, 73(5):053804, 2006.

[62] M Kozuma, D Akamatsu, Lu Deng, EW Hagley, and Marvin G Payne. Steep optical-wave group-velocity reduction and "storage" of light without on-resonance electromagnetically induced transparency. *Physical Review A*, 66(3):031801, 2002.

[63] A Mair, J Hager, DF Phillips, RL Walsworth, and MD Lukin. Phase coherence and control of stored photonic information. *Physical Review A*, 65(3):031802, 2002.

[64] David Petrosyan and Gershon Kurizki. Symmetric photon-photon coupling by atoms with zeeman-split sublevels. *Physical Review A*, 65(3):033833, 2002.

[65] M Bajcsy, Alexander S Zibrov, and Mikhail D Lukin. Stationary pulses of light in an atomic medium. *Nature*, 426(6967):638–641, 2003.

[66] Eden Figueroa, J Appel, D Korystov, M Lobino, C Kupchak, and AI Lvovsky. Electromagnetically-induced transparency and squeezed light. In *AIP Conference Proceedings*, volume 1110, pages 249–252. American Institute of Physics, 2009.

[67] Nathaniel B Phillips, Alexey V Gorshkov, and Irina Novikova. Light storage in an optically thick atomic ensemble under conditions of electromagnetically induced transparency and four-wave mixing. *Physical Review A*, 83(6):063823, 2011.

[68] P Valente, H Failache, and A Lezama. Comparative study of the transient evolution of hanle electromagnetically induced transparency and absorption resonances. *Physical Review A*, 65(2):023814, 2002.

[69] CL Garrido Alzar, LS Cruz, JG Aguirre Gómez, M França Santos, and P Nussenzveig. Super-poissonian intensity fluctuations and correlations between pump and probe fields in electromagnetically induced transparency. *Europhysics Letters*, 61(4):485, 2003.

[70] Xiao Feng, Guo Rui-Min, Chen Shuai, Zhang Yu, Li Lu-Ming, and Chen Xu-Zong. Observation of electromagnetically induced transparency in a zeeman-sublevel system in rubidium atomic vapour. *Chinese physics letters*, 20(8):1257, 2003.

[71] G Alzetta, S Gozzini, A Lucchesini, S Cartaleva, T Karaulanov, C Marinelli, and L Moi. Complete electromagnetically induced transparency in sodium atoms excited by a multimode dye laser. *Physical Review A*, 69(6):063815, 2004.

[72] PRS Carvalho, Luís EE de Araujo, and JWR Tabosa. Angular dependence of an electromagnetically induced transparency resonance in a doppler-broadened atomic vapor. *Physical Review A*, 70(6):063818, 2004.

[73] Anusha Krishna, Kanhaiya Pandey, Ajay Wasan, and Vasant Natarajan. High-resolution hyperfine spectroscopy of excited states using electromagnetically induced transparency. *Europhysics Letters*, 72(2):221, 2005.

[74] Vladimir A Sautenkov, Yuri V Rostovtsev, CY Ye, George R Welch, Olga Kocharovskaya, and Marlan O Scully. Electromagnetically induced transparency in rubidium vapor prepared by a comb of short optical pulses. *Physical Review A*, 71(6):063804, 2005.

[75] Zhi-Xiang Xu, Wei-Zhi Qu, Ran Gao, Xin-Hua Hu, and Yan-Hong Xiao. Linewidth of electromagnetically induced transparency under motional averaging in a coated vapor cell. *Chinese Physics B*, 22(3):033202, 2013.

[76] SM Ćuk, AJ Krmpot, M Radonjić, SN Nikolić, and BM Jelenković. Influence of a laser beam radial intensity distribution on zeeman electromagnetically induced transparency line-shapes in the vacuum rb cell. *Journal of Physics B: Atomic, Molecular and Optical Physics*, 46(17):175501, 2013.

[77] Xiao-Gang Wei, Jin-Hui Wu, Gui-Xia Sun, Zhuang Shao, Zhi-Hui Kang, Yun Jiang, and Jin-Yue Gao. Splitting of an electromagnetically induced transparency window of rubidium atoms in a static magnetic field. *Physical Review A*, 72(2):023806, 2005.

[78] Jianming Wen, Shengwang Du, and Morton H Rubin. Biphoton generation in a two-level atomic ensemble. *Physical Review A*, 75(3):033809, 2007.

[79] SC Bell, DM Heywood, JD White, JD Close, and RE Scholten. Laser frequency offset locking using electromagnetically induced transparency. *Applied Physics Letters*, 90(17), 2007.

[80] RP Abel, AK Mohapatra, Mark George Bason, JD Pritchard, KJ Weatherill, U Raitzsch, and CS Adams. Laser frequency stabilization to excited state transitions using electromagnetically induced transparency in a cascade system. *Applied Physics Letters*, 94(7), 2009.

[81] Aleksandar J Krmpot, Mihailo D Rabasović, and Branislav M Jelenković. Optical pumping spectroscopy of rb vapour with co-propagating laser beams: line identification by a simple theoretical model. *Journal of Physics B: Atomic, Molecular and Optical Physics*, 43(13):135402, 2010.

[82] Kanhaiya Pandey and Vasant Natarajan. Splitting of electromagnetically induced transparency under strong-probe conditions due to doppler averaging. *Journal of Physics B: Atomic, Molecular and Optical Physics*, 41(18):185504, 2008.

[83] VA Reshetov and IV Meleshko. Electromagnetically induced transparency with degenerate atomic levels. *Laser Physics*, 24(9):094011, 2014.

[84] Dipankar Bhattacharyya, Arindam Ghosh, Amitava Bandyopadhyay, Satyajit Saha, and Sankar De. Observation of electromagnetically induced transparency in six-level rb atoms and theoretical simulation of the observed spectra. *Journal of Physics B: Atomic, Molecular and Optical Physics*, 48(17):175503, 2015.

[85] A Yu Kalatskiy, AE Afanasiev, PN Melentiev, and VI Balykin. Frequency stabilization of a diode laser on the 5p→ 5d transition of the rb atom. *Laser Physics*, 27(5):055703, 2017.

[86] Kavita Yadav and Ajay Wasan. Five-and seven-level inhomogeneously broadened ξ systems with mismatched wavelengths and polarization effects. *The European Physical Journal D*, 72:1–8, 2018.

[87] U Rathe, M Fleischhauer, Shi-Yao Zhu, TW Hänsch, and MO Scully. Nonlinear theory of index enhancement via quantum coherence and interference. *Physical Review A*, 47(6):4994, 1993.

[88] AB Matsko, YV Rostovtsev, O Kocharovskaya, AS Zibrov, and MO Scully. Nonadiabatic approach to quantum optical information storage. *Physical Review A*, 64(4):043809, 2001.

[89] Yu I Geller, DE Sovkov, AT Hakim'yanov, and AV Sharypov. Dispersion properties of electromagnetically induced transparency under the doppler broadening. *Russian Physics Journal*, 50:259–266, 2007.

[90] Brzostowski Bartosz, Khoa Dinh Xuan, Grabiec Bogdan, Ngoc Sau Vu, Żaba Agnieszka, et al. Eit four-level lambda scheme of cold rubidium atoms. *CMST*, (2):13–16, 2010.

[91] OS Mishina, M Scherman, P Lombardi, J Ortalo, D Felinto, AS Sheremet, DV Kupriyanov, J Laurat, and E Giacobino. Enhancement of electromagnetically induced transparency in room temperature alkali metal vapor. *Optics and Spectroscopy*, 111:583–588, 2011.

[92] Qiong-Yi He, Xiao-Gang Wei, Jin-Hui Wu, Bing Zhang, and Jin-Yue Gao. Coherent hole-burnings induced by a bichromatic laser field. *Optics communications*, 281(11):3137–3142, 2008.

[93] Xiao-Yu Yang and Yong-Yuan Jiang. The influence of eit effect with double windows on electromagnetic characteristics of quasi-λ-four-level atomic system. *Optics Communications*, 285(8):2161–2165, 2012.

[94] Ali Raheli, M Sahrai, and HR Hamedi. Atom position measurement in a four-level lambda-shaped scheme with twofold lower-levels. *Optical and Quantum Electronics*, 47:3221–3236, 2015.

[95] Julio Gea-Banacloche, Yong-qing Li, Shao-zheng Jin, and Min Xiao. Electromagnetically induced transparency in ladder-type inhomogeneously broadened media: Theory and experiment. *Physical Review A*, 51(1):576, 1995.

[96] Yonghong Ling, Lirong Huang, Wei Hong, Tongjun Liu, Jing Luan, Wenbing Liu, Jianjun Lai, and Hanping Li. Polarization-controlled dynamically switchable plasmon-induced transparency in plasmonic metamaterial. *Nanoscale*, 10(41):19517–19523, 2018.

[97] David McGloin, DJ Fulton, and Malcolm Harry Dunn. Electromagnetically induced transparency in n-level cascade schemes. *Optics communications*, 190(1-6):221–229, 2001.

[98] Bibhas K Dutta and Prasanta K Mahapatra. Nonlinear optical effects in a doubly driven four-level atom. *Physica Scripta*, 75(3):345, 2007.

[99] HR Hamedi, Gediminas Juzeliūnas, A Raheli, and M Sahrai. High refractive index and lasing without inversion in an open four-level atomic system. *Optics Communications*, 311:261–265, 2013.

[100] M Anil Kumar and Suneel Singh. Electromagnetically induced transparency and slow light in three-level ladder systems: Effect of velocity-changing and dephasing collisions. *Physical Review A*, 79(6):063821, 2009.

[101] Hwang Lee and Marlan O Scully. The physics of eit and lwi in v-type configurations. *Foundations of physics*, 28(4):585–600, 1998.

[102] Bibhas K Dutta and Prasanta K Mahapatra. Role of incoherent pumping scheme on gain without population inversion in four-level systems. *Physica Scripta*, 77(2):025403, 2008.

[103] DG Han, YG Zeng, H Guo, W Chen, H Lu, and C Huang. Effects of the upper level coupling field on lasing without inversion in a v-type system. *The European Physical Journal D*, 42:489–493, 2007.

[104] X-M Hu, J Xiong, and J-s Peng. Spectral linewidth of inversionless and raman lasers in v-type three-level systems. *The European Physical Journal D-Atomic, Molecular, Optical and Plasma Physics*, 13:401–413, 2001.

[105] S Dey, S Mitra, PN Ghosh, and B Ray. Eit line shape in an open and partially closed multilevel v-type system. *Optik*, 126(20):2711–2717, 2015.

[106] Yoshitaka Hoshina, Nobuhito Hayashi, Kosuke Tsubota, Ichiro Yoshida, Kotaro Shijo, Ryuta Sugizono, and Masaharu Mitsunaga. Electromagnetically induced transparency in a v-type multilevel system of na vapor. *JOSA B*, 31(8):1808–1813, 2014.

[107] SM Mousavi, L Safari, M Mahmoudi, and M Sahrai. Effect of quantum interference on the optical properties of a three-level v-type atomic system beyond the two-photon resonance condition. *Journal of Physics B: Atomic, Molecular and Optical Physics*, 43(16):165501, 2010.

[108] Dong Yan, Yi-Mou Liu, Qian-Qian Bao, Chang-Bao Fu, and Jin-Hui Wu. Electromagnetically induced transparency in an inverted-y system of interacting cold atoms. *Physical Review A*, 86(2):023828, 2012.

[109] KI Osman, SS Hassan, and A Joshi. Effect of spontaneously generated coherence on eit and its refractive properties in four-and five-levels systems. *The European Physical Journal D*, 54:119–130, 2009.

[110] Jun Kou, Ren-Gang Wan, Shang-Qi Kuang, Li Jiang, Liang Zhang, Zhi-Hui Kang, Hai-Hua Wang, and Jin-Yue Gao. Double dark resonances and the dispersion properties in a four-level inverted-y atomic system. *Optics Communications*, 284(6):1603–1607, 2011.

[111] Arindam Ghosh, Khairul Islam, Dipankar Bhattacharyya, and Amitava Bandyopadhyay. Revisiting the four-level inverted-y system under both doppler-free and doppler-broadened conditions: an analytical approach. *Journal of Physics B: Atomic, Molecular and Optical Physics*, 49(19):195401, 2016.

[112] MA Antón, F Carreño, Oscar G Calderón, S Melle, and I Gonzalo. Optical switching by controlling the double-dark resonances in a n-tripod five-level atom. *Optics communications*, 281(24):6040–6048, 2008.

[113] Yi Chen, Xiao Gang Wei, and BS Ham. Optical properties of an n-type system in doppler-broadened multilevel atomic media of the rubidium d2 line. *Journal of Physics B: Atomic, Molecular and Optical Physics*, 42(6):065506, 2009.

[114] LB Kong, XH Tu, J Wang, Yifu Zhu, and MS Zhan. Sub-doppler spectral resolution in a resonantly driven four-level coherent medium. *Optics communications*, 269(2):362–369, 2007.

[115] Zhenkun Wu, Chenzhi Yuan, Zhaoyang Zhang, Huaibin Zheng, Shuli Huo, Ruyi Zhang, Ruimin Wang, and Yanpeng Zhang. Observation of eight-wave mixing via electromagnetically induced transparency. *Europhysics Letters*, 94(6):64005, 2011.

[116] Yu M Golubev, T Yu Golubeva, Yu V Rostovtsev, and MO Scully. Control of group velocity of light via magnetic field. *Optics communications*, 278(2):350–362, 2007.

[117] Julian Naber, Atreju Tauschinsky, Ben van Linden van den Heuvell, and Robert Spreeuw. Electromagnetically induced transparency with rydberg atoms across the breit-rabi regime. *SciPost Physics*, 2(2):015, 2017.

[118] Xue-Dong Tian, Yi-Mou Liu, Xiao-Bo Yan, Cui-Li Cui, and Yan Zhang. Electromagnetically induced transparency in a y system with single rydberg state. *Optics Communications*, 345:6–12, 2015.

[119] Dushmanta Kara, Arup Bhowmick, and Ashok K Mohapatra. Rydberg interaction induced enhanced excitation in thermal atomic vapor. *Scientific reports*, 8(1):5256, 2018.

[120] Le-Man Kuang and Lan Zhou. Generation of atom-photon entangled states in atomic bose-einstein condensate via electromagnetically induced transparency. *Physical review A*, 68(4):043606, 2003.

[121] RG Beausoleil, WJ Munro, DA Rodrigues, and TP Spiller. Applications of electromagnetically induced transparency to quantum information processing. *Journal of Modern Optics*, 51(16-18):2441–2448, 2004.

[122] Hui Jing, Xiong-Jun Liu, Mo-Lin Ge, and Ming-Sheng Zhan. Correlated quantum memory: Manipulating atomic entanglement via electromagnetically induced transparency. *Physical Review A*, 71(6):062336, 2005.

[123] Qingqing Sun, Yuri V Rostovtsev, and M Suhail Zubairy. Optical beam steering based on electromagnetically induced transparency. *Physical Review A*, 74(3):033819, 2006.

[124] John B Pendry, Anthony J Holden, David J Robbins, and WJ Stewart. Magnetism from conductors and enhanced nonlinear phenomena. *IEEE transactions on microwave theory and techniques*, 47(11):2075–2084, 1999.

[125] Richard A Shelby, David R Smith, and Seldon Schultz. Experimental verification of a negative index of refraction. *science*, 292(5514):77–79, 2001.

[126] Ta-Jen Yen, WJ Padilla, Nicholas Fang, DC Vier, DR Smith, JB Pendry, DN Basov, and Xiang Zhang. Terahertz magnetic response from artificial materials. *Science*, 303(5663):1494–1496, 2004.

[127] Shuang Zhang, Wenjun Fan, NC Panoiu, KJ Malloy, RM Osgood, and SRJ Brueck. Experimental demonstration of near-infrared negative-index metamaterials. *Physical review letters*, 95(13):137404, 2005.

[128] Shuang Zhang, Wenjun Fan, NC Panoiu, KJ Malloy, RM Osgood, and SRJ Brueck. Optical negative-index bulk metamaterials consisting of 2d perforated metal-dielectric stacks. *Optics Express*, 14(15):6778–6787, 2006.

[129] Stefan Linden, Christian Enkrich, Martin Wegener, Jiangfeng Zhou, Thomas Koschny, and Costas M Soukoulis. Magnetic response of metamaterials at 100 terahertz. *Science*, 306(5700):1351–1353, 2004.

[130] Vladimir M Shalaev. Optical negative-index metamaterials. *Nature photonics*, 1(1):41–48, 2007.

[131] Hsiao-Kuan Yuan, Uday K Chettiar, Wenshan Cai, Alexander V Kildishev, Alexandra Boltasseva, Vladimir P Drachev, and Vladimir M Shalaev. A negative permeability material at red light. *Optics Express*, 15(3):1076–1083, 2007.

[132] Costas M Soukoulis, Stefan Linden, and Martin Wegener. Negative refractive index at optical wavelengths. *Science*, 315(5808):47–49, 2007.

[133] Gunnar Dolling, Martin Wegener, Costas M Soukoulis, and Stefan Linden. Negative-index metamaterial at 780 nm wavelength. *Optics letters*, 32(1):53–55, 2007.

[134] M Kafesaki, I Tsiapa, N Katsarakis, Th Koschny, CM Soukoulis, and EN Economou. Left-handed metamaterials: The fishnet structure and its variations. *Physical Review B*, 75(23):235114, 2007.

[135] Ting Xu, Amit Agrawal, Maxim Abashin, Kenneth J Chau, and Henri J Lezec. All-angle negative refraction and active flat lensing of ultraviolet light. *Nature*, 497(7450):470–474, 2013.

[136] Costas M Soukoulis and Martin Wegener. Optical metamaterials—more bulky and less lossy. *Science*, 330(6011):1633–1634, 2010.

[137] Zhiguang Liu, Zhe Liu, Jiafang Li, Wuxia Li, Junjie Li, Changzhi Gu, and Zhi-Yuan Li. 3d conductive coupling for efficient generation of prominent fano resonances in metamaterials. *Scientific reports*, 6(1):27817, 2016.

[138] Pascal Macha, Gregor Oelsner, Jan-Michael Reiner, Michael Marthaler, Stephan André, Gerd Schön, Uwe Hübner, Hans-Georg Meyer, Evgeni Il'ichev, and Alexey V Ustinov. Implementation of a quantum metamaterial using superconducting qubits. *Nature communications*, 5(1):5146, 2014.

[139] Alexandre M Zagoskin, Didier Felbacq, and Emmanuel Rousseau. Quantum metamaterials in the microwave and optical ranges. *EPJ Quantum Technology*, 3(1):1–17, 2016.

[140] Lei Kang, Shoufeng Lan, Yonghao Cui, Sean P Rodrigues, Yongmin Liu, Douglas H Werner, and Wenshan Cai. An active metamaterial platform for chiral responsive optoelectronics. *Advanced Materials*, 27(29):4377–4383, 2015.

[141] Matthew Reynolds and Stephen Daley. An active viscoelastic metamaterial for isolation applications. *Smart materials and structures*, 23(4):045030, 2014.

[142] Sher-Yi Chiam, Ranjan Singh, Carsten Rockstuhl, Falk Lederer, Weili Zhang, and Andrew A Bettiol. Analogue of electromagnetically induced transparency in a terahertz metamaterial. *Physical Review B*, 80(15):153103, 2009.

[143] Sher-Yi Chiam, Ranjan Singh, Jianqiang Gu, Jiaguang Han, Weili Zhang, and Andrew A Bettiol. Increased frequency shifts in high aspect ratio terahertz split ring resonators. *Applied Physics Letters*, 94(6), 2009.

[144] Na Liu, Lutz Langguth, Thomas Weiss, Jürgen Kästel, Michael Fleischhauer, Tilman Pfau, and Harald Giessen. Plasmonic analogue of electromagnetically induced transparency at the drude damping limit. *Nature materials*, 8(9):758–762, 2009.

[145] Chao Tang, Qingshan Niu, Yuanhao He, Huaxin Zhu, and Ben-Xin Wang. Tunable triple-band plasmonically induced transparency effects based on double π-shaped metamaterial resonators. *Plasmonics*, 15:467–473, 2020.

[146] Binggang Xiao, Shengjun Tong, Alexander Fyffe, and Zhimin Shi. Tunable electromagnetically induced transparency based on graphene metamaterials. *Optics Express*, 28(3):4048–4057, 2020.

[147] Junhu Zhou, Chenxi Zhang, Qirui Liu, Jie You, Xin Zheng, Xiang'ai Cheng, and Tian Jiang. Controllable all-optical modulation speed in hybrid silicon-germanium devices utilizing the electromagnetically induced transparency effect. *Nanophotonics*, 9(9):2797–2807, 2020.

[148] WL Barnes, SC Kitson, TW Preist, and JR Sambles. Photonic surfaces for surface-plasmon polaritons. *JOSA A*, 14(7):1654–1661, 1997.

[149] Hiroshi Kano, Seiji Mizuguchi, and Satoshi Kawata. Excitation of surface-plasmon polaritons by a focused laser beam. *JOSA B*, 15(4):1381–1386, 1998.

[150] Sergey I Bozhevolnyi and Victor Coello. Elastic scattering of surface plasmon polaritons: modeling and experiment. *Physical review B*, 58(16):10899, 1998.

[151] Harald Ditlbacher, Joachim R Krenn, Gerburg Schider, Alfred Leitner, and Franz R Aussenegg. Two-dimensional optics with surface plasmon polaritons. *Applied Physics Letters*, 81(10):1762–1764, 2002.

[152] Anatoly V Zayats and Igor I Smolyaninov. Near-field photonics: surface plasmon polaritons and localized surface plasmons. *Journal of Optics A: Pure and Applied Optics*, 5(4):S16, 2003.

[153] JR Krenn and J-C Weeber. Surface plasmon polaritons in metal stripes and wires. *Philosophical Transactions of the Royal Society of London. Series A: Mathematical, Physical and Engineering Sciences*, 362(1817):739–756, 2004.

[154] A Andre, MD Eisaman, RL Walsworth, AS Zibrov, and MD Lukin. Quantum control of light using electromagnetically induced transparency. *Journal of Physics B: Atomic, Molecular and Optical Physics*, 38(9):S589, 2005.

[155] Yuehui Lu, Hua Xu, Joo Yull Rhee, Won Ho Jang, Byoung Seung Ham, and YoungPak Lee. Magnetic plasmon resonance: Underlying route to plasmonic electromagnetically induced transparency in metamaterials. *Physical Review B*, 82(19):195112, 2010.

[156] Zhihong Chen, Lei Dai, and Chun Jiang. Polarization-independent plasmon-induced transparency for plasmonic sensing. *Journal of Physics D: Applied Physics*, 44(32):325106, 2011.

[157] Chunguang Du, Qingli Jing, and Zhengfeng Hu. Coupler-free transition from light to surface plasmon polariton. *Physical Review A*, 91(1):013817, 2015.

[158] Tengfei Meng, Yanting Zhao, Zhonghua Ji, Dianqiang Su, Liantuan Xiao, and Suotang Jia. V-type electromagnetically induced transparency and saturation effect at the gas-solid interface. *arXiv preprint arXiv:1503.04950*, 2015.

[159] Saeed Asgarnezhad-Zorgabad, Rasoul Sadighi-Bonabi, and Chao Hang. Coupler-free surface polariton excitation and propagation with cold four-level atomic medium. *JOSA B*, 34(9):1787–1795, 2017.

[160] Saeid Asgarnezhad-Zorgabad, Rasoul Sadighi-Bonabi, and Barry C Sanders. Excitation and propagation of surface polaritonic rogue waves and breathers. *Physical Review A*, 98(1):013825, 2018.